Tectonostratigraphic evolution of the *c.* 780–730 Ma Beck Spring Dolomite: Basin Formation in the core of Rodinia

EMILY F. SMITH[1]*, FRANCIS A. MACDONALD[1], JAMES L. CROWLEY[2], EBEN B. HODGIN[1] & DANIEL P. SCHRAG[1]

[1]*Department of Earth and Planetary Sciences, Harvard University, Cambridge, MA 02138, USA*

[2]*Department of Geosciences, Boise State University, Boise, ID 83725, USA*

**Corresponding author (e-mail: efsmith@fas.harvard.edu)*

Abstract: The Beck Spring Dolomite is a mixed carbonate–siliciclastic succession exposed in Death Valley, California, that was deposited between 780 and 717 Ma. Along with its bounding units, the Horse Thief Springs Formation below and unit KP1 of the Kingston Peak Formation above, the Beck Spring Dolomite were deposited in one of the ChUMP (Chuar–Uinta Mountains–Pahrump) basins with subsidence commonly attributed to the nascent rifting of Rodinia. These pre-Sturtian successions preserve eukaryotic microfossil assemblages, diverse microbialites, and large carbon isotope anomalies directly below Sturtian-age glacial deposits. Here we present new geological mapping, measured stratigraphic sections, carbon isotope chemostratigraphy and detrital zircon geochronology from the Beck Spring Dolomite and its bounding units. The carbon isotope excursion at the top of the Beck Spring Dolomite has previously been attributed to meteoric diagenesis associated with karst breccias, but here we demonstrate that these breccias are instead mass flow deposits that formed during deposition of the Kingston Peak Formation and that the carbon isotope excursion is not only reproducible throughout the basin, but is associated with transgression rather than regression and exposure. In addition, we refine local correlations and discuss the use of chemostratigraphic curves from these units for regional and global correlations. The Beck Spring Dolomite was deposited during the second of three distinct basin-forming events recorded in the Pahrump Group with basin inversion occurring between each event. The presence of syn-sedimentary faults, the character of the lateral facies change and detrital zircon provenance analyses indicate that the Beck Spring Dolomite fringed a coeval palaeo-high to the south in a tectonically active basin. Detrital zircon age distributions in the Beck Spring Dolomite show sharp probability peaks at *c.* 1200, 1400 and 1800 Ma, consistent with local sources to the SW in the Mojave block rather than transcontinental rivers. The *c.* 1800 Ma probability peak is less prominent in the KP1 samples. In addition, KP1 also records slump folding and is overlain by an unconformity. We suggest that these features are consistent with the emergence of a local fault to the NE. Deposition of the Beck Spring Dolomite and bounding units do not record evidence of incipient rifting of the western margin of Laurentia but instead reflect a distinct and separate tectonothermal event.

Supplementary material: Carbon ($\delta^{13}C$) and oxygen ($\delta^{18}O$) isotopic measurements, detrital zircon laser ablation inductively coupled plasma mass spectrometry (LA-ICPMS) data, detrital zircon sample information and data from reference materials used for LA-ICPMS analyses are available at http://www.geolsoc.org.uk/SUP18823.

The Death Valley region of SE California hosts a 1.5–4.0 km-thick, well-exposed Neoproterozoic succession, the Pahrump Group (Figs 1 & 2). The classic view is that the three units comprising the group, the Crystal Spring Formation, Beck Spring Dolomite and Kingston Peak Formation, formed in a long-lived aulacogen bounded to the north and south by upland source areas, and that carbonate-dominated units like the Beck Spring Dolomite were deposited during periods of tectonic quiescence (Wright *et al.* 1976; Roberts 1982). This model was developed when there were few age constraints on these strata. Nearly a decade later, researchers used ages of basement terrains, Grenville-age orogenic belts and stratigraphic ties to hypothesize the formation and break-up of the supercontinent Rodinia (Dalziel 1991; Hoffman 1991; Moores 1991). Details of the palaeogeographic arrangement and components of Rodinia are still debated, but nearly all models place Laurentia at the core of the supercontinent. Thus, Neoproterozoic basin formation in Death Valley is especially important for the reconstruction of Rodinia because it was proximal to both the western and southern margins of Laurentia, and as a result, has the potential to record the tectonic evolution

From: Li, Z. X., Evans, D. A. D. & Murphy, J. B. (eds) *Supercontinent Cycles Through Earth History*. Geological Society, London, Special Publications, **424**, http://doi.org/10.1144/SP424.6

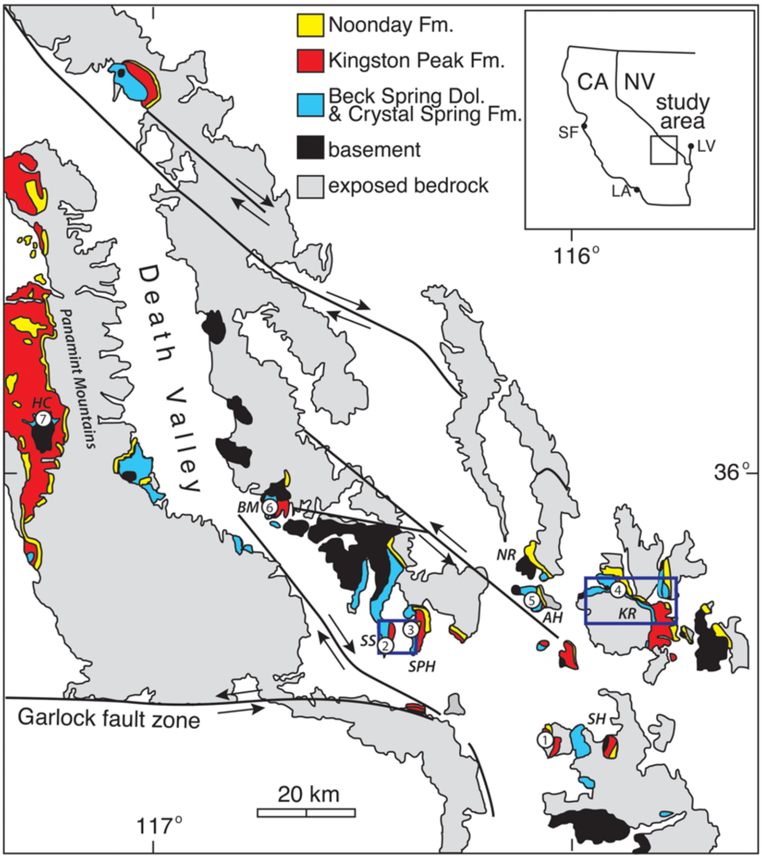

Fig. 1. Location map and major faults. AH, Alexander Hills; BM, lack Mountains; HC, Happy Canyon; KR, Kingston Range; NR, Nopah Range; SH, Silurian Hills; SPH, Saddle Peak Hills; SS, Saratoga Springs (southern Ibex Hills); and SW, Sperry Wash. The areas mapped in Figures 3 and 4 are boxed in blue. Locations of measured sections are marked with circled numbers that correspond to numbered sections in Figure 5.

of both margins. Over the past few decades, age constraints have been refined and several major unconformities have been recognized within the Pahrump Group, suggesting that the strata were deposited during multiple, distinct basin-forming events and, thus calling into question the long-lived aulacogen model (Heaman & Grotzinger 1992; Prave 1999; Macdonald *et al.* 2013*a*; Mahon *et al.* 2014*b*).

Other western Laurentian successions have been previously attributed to record the rifting of Rodinia, including the Chuar Group in Arizona (Timmons *et al.* 2001) and the Uinta Mountain Group in Utah (Dehler *et al.* 2010). These basins are collectively referred to as the ChUMP (Chuar–Uinta Mountains–Pahrump) basins, and are thought to have formed in an extensive interior seaway that formed in the incipient stages of rifting (Link 1993; Dehler *et al.* 2001, 2010). The shared features between units in the ChUMP basins include similar fossil assemblages with vase-shaped microfossils (VSMs) in the uppermost stratigraphy (Licari 1978; Porter & Knoll 2000; Dehler *et al.* 2010), unconformity-bounded successions with age constraints between *c.* 780 and 730 Ma (Macdonald *et al.* 2013*a*; Mahon *et al.* 2014*b*), large carbon isotope anomalies (Corsetti & Kaufman 2003; Dehler *et al.* 2005, 2007, 2010; Brehm 2008; Macdonald *et al.* 2013*a*) and pronounced metre-scale cyclicity (Dehler *et al.* 2001). Similar features and age constraints also have been documented in the Callison Lake dolostone and Coates Lake Group of NW Canada (Jefferson & Parrish 1989; Macdonald *et al.* 2010; Rooney *et al.* 2014; Strauss *et al.* 2014).

Here, with new and previously published data, we propose an alternative model for the tectonostratigraphic evolution and subsidence mechanisms for the iconic Pahrump Group in Death Valley. This new model integrates geological mapping, measured sections, detrital zircon geochronology and carbon isotope chemostratigraphy of the Beck Spring Dolomite and its encasing strata, the underlying Horse Thief Springs Formation (previously defined as the upper member of the Crystal Spring Formation) and the overlying unit KP1 of the Kingston Peak Formation (Macdonald *et al.* 2013*a*; Mahon *et al.* 2014*b*) from seven localities (Fig. 1). These strata are bounded by unconformities, which Macdonald *et al.* (2013*a*) used to demarcate Tectonostratigraphic Unit 2 (TU2), a regionally developed package interpreted to record a distinct basin-forming event. To avoid nomenclatural issues, we will use TU2 throughout to delineate this succession of rocks.

Geological setting

In Death Valley, the Pahrump Group defines a 1.5–4.0 km-thick, well-exposed and easily accessible Meso- and Neoproterozoic succession (Noble 1934; Hewett 1940). Its basal unit, the Crystal Spring Formation, unconformably overlies 1780–1660 Ma granitic gneisses of the Mojave crustal province (Wasserburg *et al.* 1959; Barth *et al.* 2000; Strickland *et al.* 2013) and 1430–1400 Ma porphyritic quartz monzonite (Labotka *et al.* 1980). Following the amalgamation of the Mojave basement by 1210–1180 Ma with the intrusion of the AMCG suite of anorthosite, syenite and granite (Wooden *et al.* 2013), the Death Valley region experienced extension and basin formation. This extension accommodated the emplacement of diabase sills that have been dated at two localities at 1087 ± 3 and 1069 ± 3 Ma with discordant multi-grain baddeleyite U–Pb thermal ionization mass spectrometry (TIMS) ages (Heaman & Grotzinger 1992).

A maximum age constraint on the middle portion of the Pahrump Group (TU2) is provided by the Crystal Spring Diabase. An upper age constraint is provided by the Noonday Formation, the basal member of which has been identified as a basal Ediacaran cap dolostone (Petterson *et al.* 2011) and has been dated globally at *c.* 635 Ma (Hoffmann *et al.* 2004; Condon *et al.* 2005; Calver *et al.* 2013). Additionally, the Kingston Peak Formation contains glacial deposits that have been correlated to the Sturtian and Marinoan glaciations (Prave 1999; Macdonald *et al.* 2010, 2013*a*). Neoproterozoic laser ablation inductively coupled plasma mass spectrometry (LA-ICPMS) detrital zircon ages (Mahon *et al.* 2014*b*) and correlation of pre-Sturtian basins on the western margin of Laurentia suggest a more narrow window of deposition of TU2 between *c.* 780 and 730 Ma (Dehler *et al.* 2001; Macdonald *et al.* 2013*a*; Strauss *et al.* 2014).

Multiple episodes of late Neoproterozoic tectonism are recorded in the Pahrump succession; evidence includes syn-sedimentary normal faults in the middle (KP2) and upper (KP3) parts of the Kingston Peak Formation in SE Death Valley, mafic dykes and basalts in the KP2- or KP3-correlative Surprise diamictite in the Panamint Mountains (Miller 1985; Prave 1999; Macdonald *et al.* 2013*a*) and multiple unconformities throughout the succession, including the base of the Noonday Formation, which regionally sits on all of the underlying units, including basement (Wright 1954; Stewart 1975; Prave 1999). Map relations and flute casts indicate that the deepening direction during Kingston Peak time was to the SSE (Mrofka 2010; Petterson *et al.* 2011). Unconformities are also present in the overlying Ediacaran strata, most prominently at the base of and in the uppermost Johnnie Formation (Summa 1993; Clapham & Corsetti 2005; Petterson *et al.* 2011). Based on subsidence curves, passive margin sedimentation did not develop in this area until latest Ediacaran–early Cambrian Wood Canyon time (Stewart 1970; Armin & Mayer 1983; Bond & Kominz 1984; Bond *et al.* 1985; Fedo & Cooper 2001). This passive margin was deepening to the NW (Nelson 1978). Thus, while there is clear evidence for Ediacaran-age rifting, it remains unclear if deposition of TU2 was accommodated by rifting, transtension, transpression, compression or dynamic subsidence.

Previous studies

Until recently, the Horse Thief Springs Formation, the basal unit of TU2, was included in the Crystal Spring Formation. The base of the Horse Thief Springs Formation is marked by a significant unconformity that was first recognized by Mbuyi & Prave (1993). Mahon *et al.* (2014*b*) elevated the succession between this unconformity and the Beck Spring Dolomite to the formation level and renamed it the Horse Thief Springs Formation.

The sedimentology, stratigraphy and regional depositional patterns of the Horse Thief Springs Formation were documented by Maud (1979, 1983), Roberts (1982) and Mahon (2012). Maud (1979, 1983) separated the unit into six regionally traceable sequences of dominantly siliciclastic rocks that are each overlain by dolomite, with the final sequence being overlain by the Beck Spring Dolomite. He labelled these sequences A–F, as shown on the left side of the Beck Canyon section in Figure 5. The lower part of the formation preserves enterolithic bedding, which Maud interpreted as evidence for deposition of evaporites in a restricted

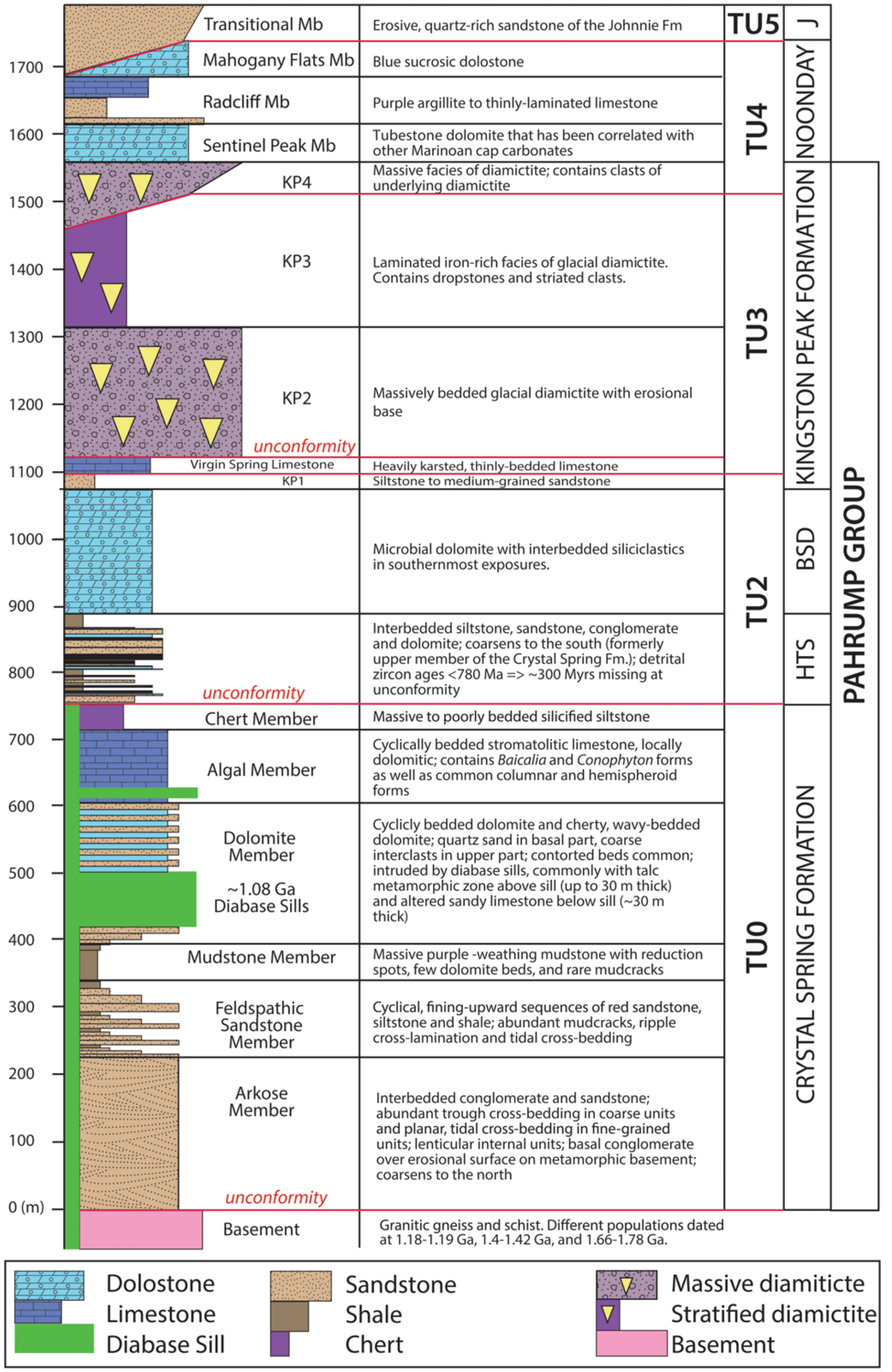
Transitional Mb
Erosive, quartz-rich sandstone of the Johnnie Fm
TU5
J
1700
Mahogany Flats Mb
Blue sucrosic dolostone
Radcliff Mb
Purple argillite to thinly-laminated limestone
1600
Sentinel Peak Mb
Tubestone dolomite that has been correlated with other Marinoan cap carbonates
TU4
NOONDAY
KP4
Massive facies of diamictite; contains clasts of underlying diamictite
1500
KP3
Laminated iron-rich facies of glacial diamictite. Contains dropstones and striated clasts.
1400
1300
KP2
Massively bedded glacial diamictite with erosional base
1200
unconformity
Virgin Spring Limestone
Heavily karsted, thinly-bedded limestone
1100
KP1
Siltstone to medium-grained sandstone
TU3
KINGSTON PEAK FORMATION
1000
Microbial dolomite with interbedded siliciclastics in southernmost exposures.
BSD
900
Interbedded siltstone, sandstone, conglomerate and dolomite; coarsens to the south (formerly upper member of the Crystal Spring Fm.); detrital zircon ages <780 Ma => ~300 Myrs missing at unconformity
800
unconformity
HTS
TU2
PAHRUMP GROUP
Chert Member
Massive to poorly bedded silicified siltstone
700
Algal Member
Cyclically bedded stromatolitic limestone, locally dolomitic; contains Baicalia and Conophyton forms as well as common columnar and hemispheroid forms
600
Dolomite Member
~1.08 Ga Diabase Sills
Cyclicly bedded dolomite and cherty, wavy-bedded dolomite; quartz sand in basal part, coarse interclasts in upper part; contorted beds common; intruded by diabase sills, commonly with talc metamorphic zone above sill (up to 30 m thick) and altered sandy limestone below sill (~30 m thick)
500
400
Mudstone Member
Massive purple -weathing mudstone with reduction spots, few dolomite beds, and rare mudcracks
300
Feldspathic Sandstone Member
Cyclical, fining-upward sequences of red sandstone, siltstone and shale; abundant mudcracks, ripple cross-lamination and tidal cross-bedding
200
Arkose Member
Interbedded conglomerate and sandstone; abundant trough cross-bedding in coarse units and planar, tidal cross-bedding in fine-grained units; lenticular internal units; basal conglomerate over erosional surface on metamorphic basement; coarsens to the north
100
unconformity
0 (m)
TU0
CRYSTAL SPRING FORMATION
Basement
Granitic gneiss and schist. Different populations dated at 1.18-1.19 Ga, 1.4-1.42 Ga, and 1.66-1.78 Ga.
Dolostone
Limestone
Diabase Sill
Sandstone
Shale
Chert
Massive diamiticte
Stratified diamictite
Basement

basin. He also documented karsting on the top surfaces of the dolomite marker beds. The formation coarsens to the SSW and is thickest in the NW part of the Kingston Range, thinning in all directions from there (Maud 1979, 1983). Maud suggested that the facies character of the interbedded stromatolitic dolostone, siltstone, sandstone and conglomerate record near-shore marine environments. Mahon *et al.* (2014*a*) used stratigraphic and detrital zircon data to argue that the Horse Thief Springs Formation marks the intial basin development during the incipient rifting of Rodinia. The only published $\delta^{13}C$ data from the Horse Thief Springs Formation is low-resolution (10–20 m) $\delta^{13}C$ data from the upper part of the formation in Beck Canyon and at Saratoga Springs (Corsetti & Kaufman 2003).

Previous studies of the Beck Spring Dolomite focused on the petrology, sedimentology and stratigraphy of the microbial, carbonate-dominated successions of the Beck Spring Dolomite in the Kingston Range and southern Death Valley area (Gutstadt 1968; Shafer 1983; Marian & Osborne 1992; Loyd & Corsetti 2010; Harwood & Sumner 2011, 2012). In the Alexander Hills and the Kingston Range, the Beck Spring Dolomite is divided into informal submembers that include a lower laminated facies, a middle microbial, thrombolitic and intraclastic facies, and an upper cherty grainstone facies (Marian 1979; Marian & Osborne 1992; Corsetti & Kaufman 2003; Harwood & Sumner 2011). The SW exposures of the Beck Spring Dolomite contain significant siliciclastic components preserved in metre-scale parasequences, syn-depositional faults and soft-sedimentary deformation (Marian 1979; Mahon 2012; Macdonald *et al.* 2013*a*).

Much detailed work has been done to compare modern microbialites to the Beck Spring Dolomite stromatolites and thrombolites to constrain specific depositional environments, and generally, previous workers have suggested that the unit was deposited on a stable, shallow marine platform in a subtidal to intertidal environment (Marian 1979; Zempolich *et al.* 1988; Marian & Osborne 1992; Harwood & Sumner 2011). Marian (1979) suggested that this unit was deposited during a period of relatively slow and stable subsidence based on his documentation of a uniform thickness of the unit; however, much of this work only documented the carbonate-dominated sections of the Beck Spring Dolomite. Mahon (2012) and Mahon *et al.* (2014*a*) later argued that the Horse Thief Springs Formation and conformably overlying Beck Spring Dolomite were deposited in a basin that was undergoing extensional tectonism.

Carbon isotope chemostratigraphy of the Beck Spring Dolomite was documented in Alexander Hills, the Kingston Range, Saddle Peak Hills and Saratoga Springs by Corsetti & Kaufman (2003), Prave (1999) and Macdonald *et al.* (2013*a*). All of these sampled sections show a ‘W-shape’ chemostratigraphic profile with a large negative carbon isotope excursion at the top of the Beck Spring Dolomite. This excursion has been correlated with the Islay excursion (Hoffman *et al.* 2012; Strauss *et al.* 2014). Hurtgen *et al.* (2004) complemented these carbon isotope studies with a carbonate-associated sulphate isotope study.

The diagenetic history of the carbonate rocks in the Beck Spring Dolomite was described by Tucker (1982, 1983), Zempolich *et al.* (1988), Kenny & Knauth (2001), and Horodyski & Knauth (1994). The latter two studies describe palaeokarst pits containing putative microfossils and brecciated clasts with highly depleted $\delta^{13}C$ values in the Beck Spring Dolomite in the Kingston Range. Importantly, the breccia at the top of the Beck Spring Dolomite is distinct from the intraformational, intraclastic breccia that was documented in the Alexander Hills and Kingston Range (Harwood & Sumner 2011 and references therein). Horodyski & Knauth (1994) use this Beck breccia and putative microfossils as evidence for terrestrial biota during the Precambrian. Elaborating on this interpretation, Kenny & Knauth (2001) found that depleted carbon and oxygen isotope values were limited to breccia in the eastern Kingston Range. This interpretation is important because it has fuelled not only speculation about the colonization of land, but also the idea that the carbon isotope chemostratigraphy of the Beck Spring Dolomite is compromised by meteoric diagenesis and cannot be used for correlation or interpretation of the Neoproterozoic carbon cycle (e.g. Knauth & Kennedy 2009).

Undisputed microfossils from the chert and dolomite in the upper part of the Beck Spring Dolomite were described by Cloud *et al.* (1969), Licari (1978) and Pierce & Cloud (1979). These microfossils, especially VSMs, are significant because, since the early reports of them in Death Valley, they have only been found in TU2-correlative basins and identified as a potential tool for correlation (Bloeser 1985; Vidal & Ford 1985; Porter & Knoll

Fig. 2. Schematic stratigraphy of the Pahrump Group in SE Death Valley. Stratigraphy of the Crystal Spring Formation is modified from Roberts (1982). Basement age populations are from Wooden *et al.* (2013). Tectonostratigraphic unit divisions are from Macdonald *et al.* (2013*a*). HTS, Horse Thief Springs Formation; BSD, Beck Spring Dolomite; J, Johnnie Formation.

2000; Dehler *et al.* 2007), and particular assemblages have been suggested as possible Neoproterozoic index fossils (Strauss *et al.* 2014).

Overlying the Beck Spring Dolomite is unit KP1, the least studied of the three units in TU2. Historically, KP1 has been placed within the Kingston Peak Formation, owing in part to difficulty correlating the glacial stratigraphy in SE Death Valley to that in the Panamint Mountains (Wright 1954). KP1 consists of siltstone to fine-grained quartz–arkosic sandstone without glaciogenic features. Its gradational contact with the underlying Beck Spring Dolomite (Miller 1985; Wright *et al.* 1992; Mrofka 2010) and the unconformity at its top surface (Mrofka 2010; Macdonald *et al.* 2013*a*) indicate that it is part of the same basin-forming event as the Beck Spring Dolomite (Prave 1999). When the Pahrump Group stratigraphy is further refined and formalized, we support Mrofka's (2010) suggestion that unit KP1 be renamed and removed from the Kingston Peak Formation.

In addition to studies of the three TU2 units, we refer to and expand upon the geological mapping and unit descriptions of Kupfer (1960) from the Silurian Hills. More specifically, we refer to his units 4–12, which we correlate with TU2 strata (shown on the left side of the Silurian Hills section in Fig. 5).

Methods

Fieldwork

We mapped the geology and measured stratigraphic sections of TU2 in the Alexander Hills, southern Black Mountains, eastern Kingston Range, central Panamint Mountains, Saddle Peak Hills, Saratoga Springs and Silurian Hills (Figs 1, 3 & 4). TU2 is also exposed in the Funeral Range of northern Death Valley (Fig. 1); however, there, the metamorphic grade is too high to preserve sedimentary textures and meaningful stratigraphic thicknesses. Locations were selected with the aim of constructing a basin-wide depositional model across the Death Valley region. The measured sections in Figure 5 are a combination of new and previously published data.

Measured sections and carbon isotopes from Beck Canyon in the Kingston Range and the Saddle Peak Hills were previously published in Macdonald *et al.* (2013*a*); however, these sections were remeasured for this study to more closely examine the sedimentology and to better characterize the $\delta^{13}C$ values in the transition beds between the Horse Thief Springs Formation and Beck Spring Dolomite. Also of note is that, north of Beck Canyon, the Beck Spring Dolomite is the prominent ridge former (Fig. 4), and the top of the section is a very steep dip slope, preventing the measurement of a continuous section. The section in Figure 5 is a composite from three localities in Beck Canyon (Fig. 4). The $\delta^{13}C$ data from the top 27 m of the section was sampled from a fault block in the far western part of the canyon that preserves the oncoids at the top of the Beck Spring Dolomite (Fig. 7d). The upper contact with KP1 was used as a tie point between the measured sections. Owing to the dip slope and the uncertainty in correlating between sections, the thickness of the section presented in Figure 5 could be inaccurate by up to 30 m (see Fig. 5 break in section). The sedimentology of the Beck Spring Dolomite at the Alexander Hills section is modified from Harwood & Sumner (2011) and the carbon isotope values are from Corsetti & Kaufman (2003). All other data presented here are new.

Mass spectrometry

To test regional and global correlations, we sampled carbonate rocks spanning TU2 from all measured sections. Carbon ($\delta^{13}C$) and oxygen ($\delta^{18}O$) isotopic measurements were obtained on 466 samples. Samples were microdrilled along individual laminations, where visible, to obtain 5–20 mg of carbonate powder; veins, fractures and siliciclastic-rich areas were avoided. Carbonate $\delta^{13}C$ and $\delta^{18}O$ data were acquired simultaneously on a VG Optima dual inlet mass spectrometer in the Harvard University Laboratory for Geochemical Oceanography. Carbonate samples were reacted with orthophosphoric acid using a VG Isocarb preparation device, which includes a common acid bath with a magnetic stirrer. Approximately 1 mg of each sample was reacted in the bath at 90 °C. Evolved CO_2 was collected cryogenically and analysed using an in-house reference gas. Potential memory effects resulting from partially unreacted samples in the common acid-bath system were minimized by increasing the reaction time for dolomite samples. Memory effect is estimated at <0.1‰ based on variability of standards run after dolomite samples. Standard deviation (1σ) from standards was better than $\pm$0.1‰ for both $\delta^{13}C$ and $\delta^{18}O$. Carbonate $\delta^{13}C$ and $\delta^{18}O$ isotopic results are reported in per mil notation relative to V-PDB (Vienna-Pee Dee Belemnite) using an in-house Cararra Marble standard that was calibrated against several NBS carbonate standards and cross-calibrated with other laboratories.

Detrital zircon geochronology

To better constrain sedimentary provenance, 17 samples through TU2 and TU3 (which includes KP2 and KP3) were collected and 1522 zircon

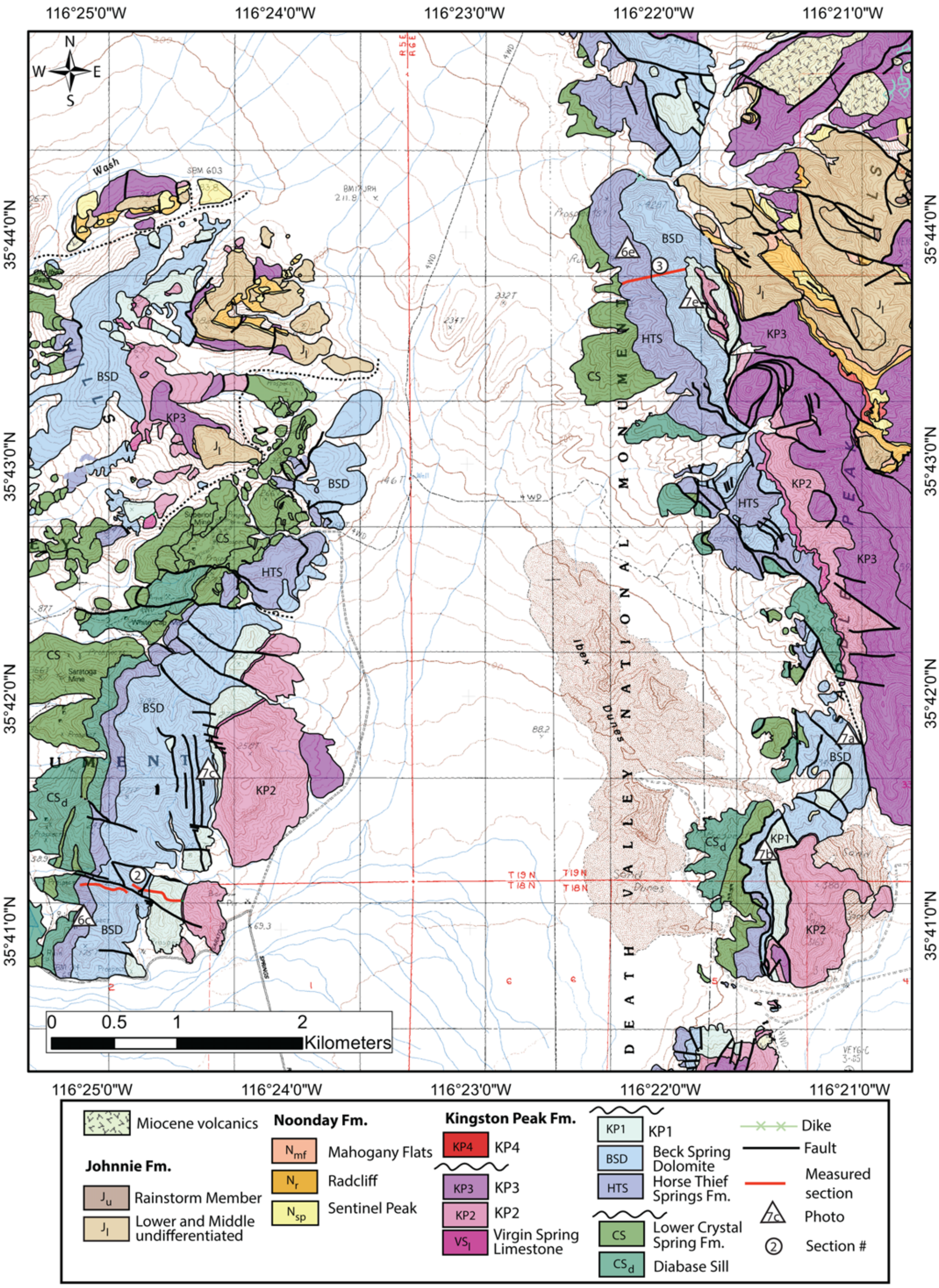

Fig. 3. Geological map of Saratoga Springs and Saddle Peak Hills. This area was mapped by F. Macdonald, E. Smith and the Harvard Field Camp in 2012 and 2013, on the Old Ibex Pass and Saddle Peak Hills 1:24 000 topographic maps with UTM gridlines. Coordinates are marked with crosses and measured sections are marked with red lines. White circles mark locations of measured sections in Figure 5. White triangles mark locations of photos in Figures 6 and 7.

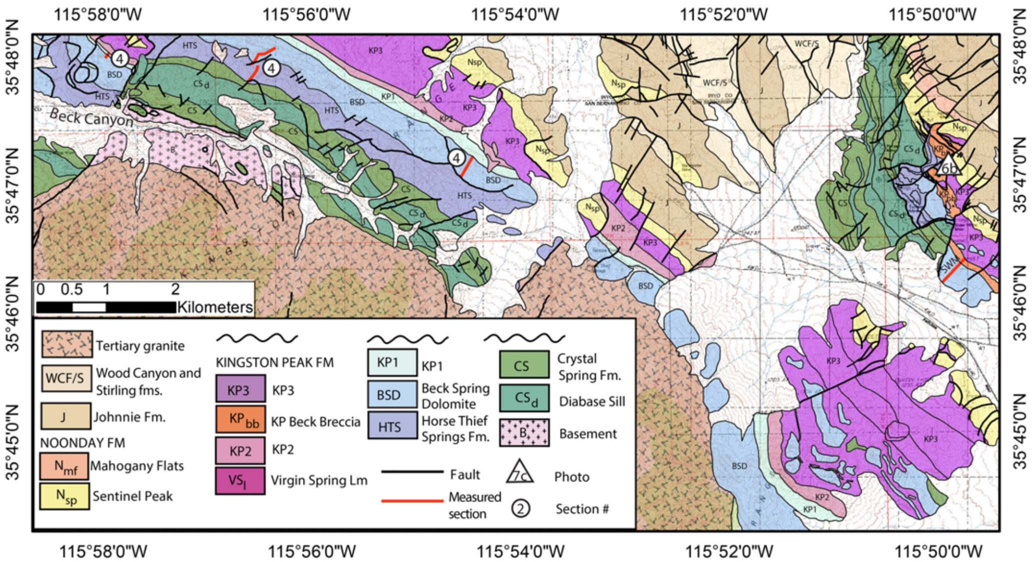

Fig. 4. Geological map of the NE Kingston Range, adapted from Calzia *et al*. (2000), Macdonald *et al.* (2013*a*), and an unpublished MIT field camp class map, courtesy of C. Burchfiel. The Crystal Spring Formation through the Kingston Peak Formation was re-mapped by F. Macdonald and E. Smith on the Horse Thief Springs and East of Kingston Peak 1:24 000 topographic maps with UTM gridlines. Coordinates are marked with crosses. White circles mark locations of measured sections in Figure 5. White triangles mark locations of photos in Figures 6 and 7. Section SWM is the location of the measured section of Beck Spring Dolomite in Harwood & Sumner (2011).

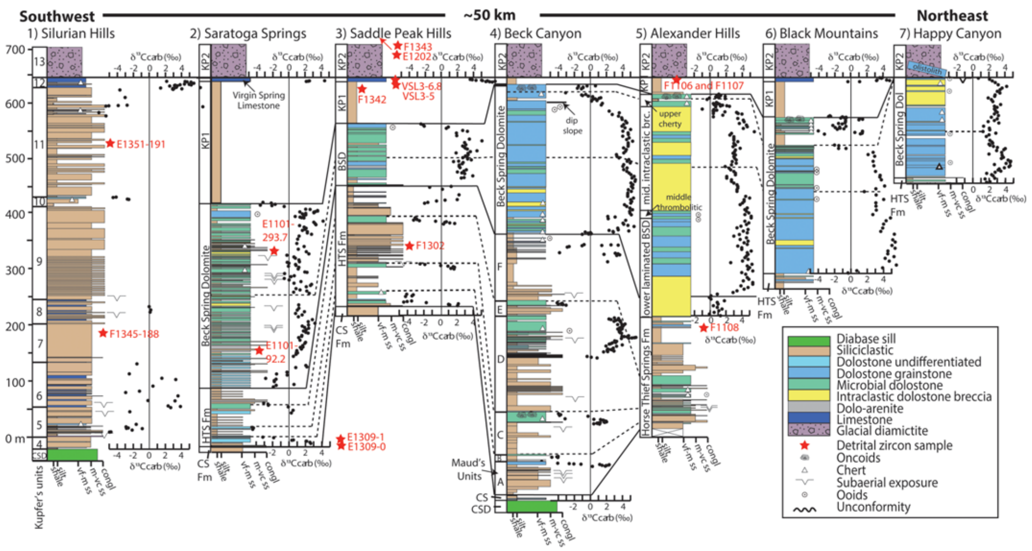

Fig. 5. Chemo- and litho-stratigraphy of TU2 from seven measured sections in SE Death Valley and the Panamint Range. See Figures 1, 3 and 4 for location maps of sections. Kupfer's (1960) units for the Silurian Hills section are marked on the left side of the section. Similarly, the members described by Maud (1979, 1983) are marked on the left side of the Horse Thief Springs Formation section in Beck Canyon and lithofacies described by Harwood & Sumner (2011) are on the left side of the Beck Spring Dolomite section at Alexander Hills. The $\delta^{13}C$ values from the Virgin Spring Limestone and Beck Spring Dolomite sections in Beck Canyon, the Black Mountains and Saddle Peak Hills were published in Macdonald *et al.* (2013*a*). In Alexander Hills, the sedimentology of the Beck Spring Dolomite is adapted from Harwood & Sumner (2011) and the $\delta^{13}C$ values are from Corsetti & Kaufman (2003). Correlation between the Silurian Hills sections and the other sections is uncertain so no tie lines are drawn. Detrital zircon samples are marked with red stars.

grains were analysed from the Pahrump Group, targeting specifically the units in TU2. These studies complement those of MacLean *et al.* (2009) and Mahon *et al.* (2014*a*, *b*). Detrital zircons were dated to assess the changes in provenance during basin development (Fig. 8b) and to find additional young (*c.* 780 Ma) grains (Mahon *et al.* 2014*b*). Samples E1309-0 and B1303 (both from the basal Horse Thief Springs Formation) were processed to search for young grains, and thus the data from these two samples are not plotted in Figure 8b, but can be found in the supplementary material. The sections and stratigraphic positions of the samples are indicated in Figure 5 with the exception of F1102 and B1303, which are from Sperry Wash and east Kingston Range, respectively.

Zircons from *c.* 2–5 kg of rock were separated using standard methods and annealed at 900 °C for 60 h. A random split of these grains (*c.* 100–200) was mounted in epoxy and polished until the centres of the grains were exposed. Cathodoluminescence (CL) images were obtained with a Jeol JSM-1300 scanning electron microscope and Gatan MiniCL. Zircons were analysed by LA-ICPMS using a ThermoElectron X-Series II quadrupole ICPMS and New Wave Research UP-213 Nd:YAG UV (213 nm) laser ablation system. In-house analytical protocols, standard materials and data reduction software were used for acquisition and calibration of U–Pb dates and a suite of high-field-strength elements and rare-earth elements. A detailed description of the methods and analyses can be found in the supplementary material.

Results

Chemo- and litho-stratigraphy

Horse Thief Springs Formation. The Horse Thief Springs Formation is a 105–465 m-thick, mixed siliciclastic–carbonate succession. For mapping purposes, we defined four regionally traceable siliciclastic–carbonate members in this formation, lumping Maud's (1979, 1983) A and B members and C and D members together (see Fig. 5); the basal three members are each capped by stromatolitic dolostone marker beds whereas the fourth member is capped by the orange and black dolostone interbedded with siltstone and fine-grained sandstone. The transition into the overlying Beck Spring Dolomite is gradational. The contact is placed at the base of the 'bacon beds', two 0.1–0.5 m-thick orange and black, microbial dolostone beds marking the onset of metre-scale mixed siliciclastic–carbonate parasequences that persist through the basal part of the Beck Spring Dolomite (see Fig. 6e for the contact at the section in western Saddle Peak Hills).

The siliciclastic strata in the Horse Thief Springs Formation include purple and green argillite, texturally immature quartz arenite, locally arkosic and poorly sorted, quartzitic conglomerate. The thicknesses and grain sizes of these strata vary widely from section to section. There are multiple exposure surfaces throughout the succession marked by mudcracks and carbonate dissolution on the upper surfaces of the dolomite beds. The carbonate rocks, often preserving *Baicalia* stromatolites, cap each of the clastic sequences across the basin (Cloud & Semikhatov 1969; Maud 1979, 1983).

Of the five new measured sections of the Horse Thief Springs Formation presented here, four were sampled for $\delta^{13}C$ analyses, providing the first high-resolution $\delta^{13}C$ dataset for these strata. Carbonate carbon isotope trends are stratigraphically consistent across the basin (Fig. 5). At Beck Canyon, the thickest and most carbonate-rich section measured, the basal carbonate units trend from *c.* +2.5 to −4.5‰. In the middle of the section, an interval that is dominated by dolomite for *c.* 80 m, there is a rise in $\delta^{13}C$ values from *c.* 0 to +6‰ and then a decrease to *c.* −4.5‰. Similar trends are present in the relatively carbonate-poor Saddle Peak Hills and Saratoga Springs sections (Fig. 5).

A siliciclastic-dominated section in the Silurian Hills that is unconformably above the Crystal Spring Formation and Crystal Spring Diabase was also measured. Owing to considerable facies changes and an upper greenschist facies overprint (Shafer 1983), detailed lithological and chemostratigraphic correlations between this section and other TU2 sections remain unclear.

Beck Spring Dolomite. The Saratoga Springs section consists of 320 m of interbedded dolostone, siltstone, sandstone and pebble conglomerate. The section is dominated by metre-scale carbonate–siliciclastic parasequences with pronounced cyclic appearance (Fig. 6c). Dolostone in the lower *c.* 100 m preserves microbial textures interbedded with finely laminated micrite, carbonate siltstone, sandstone and minor quartz–arenite pebble conglomerate. The quartz–pebble arkosic sandstone and conglomerate beds have rounded to subrounded clasts and preserve flat laminations and trough cross-bedding. Microbial laminations commonly envelop trapped quartz and feldspar grains. Sandstone beds are lobate, pinching and swelling laterally, but often continuous for hundreds of metres along strike. Broken microbial mats and millimetre- to centimetre-scale carbonate clasts are common throughout the section. At *c.* 120 m, exposure surfaces consisting of teepee structures and millimetre-scale karsting become common, suggesting

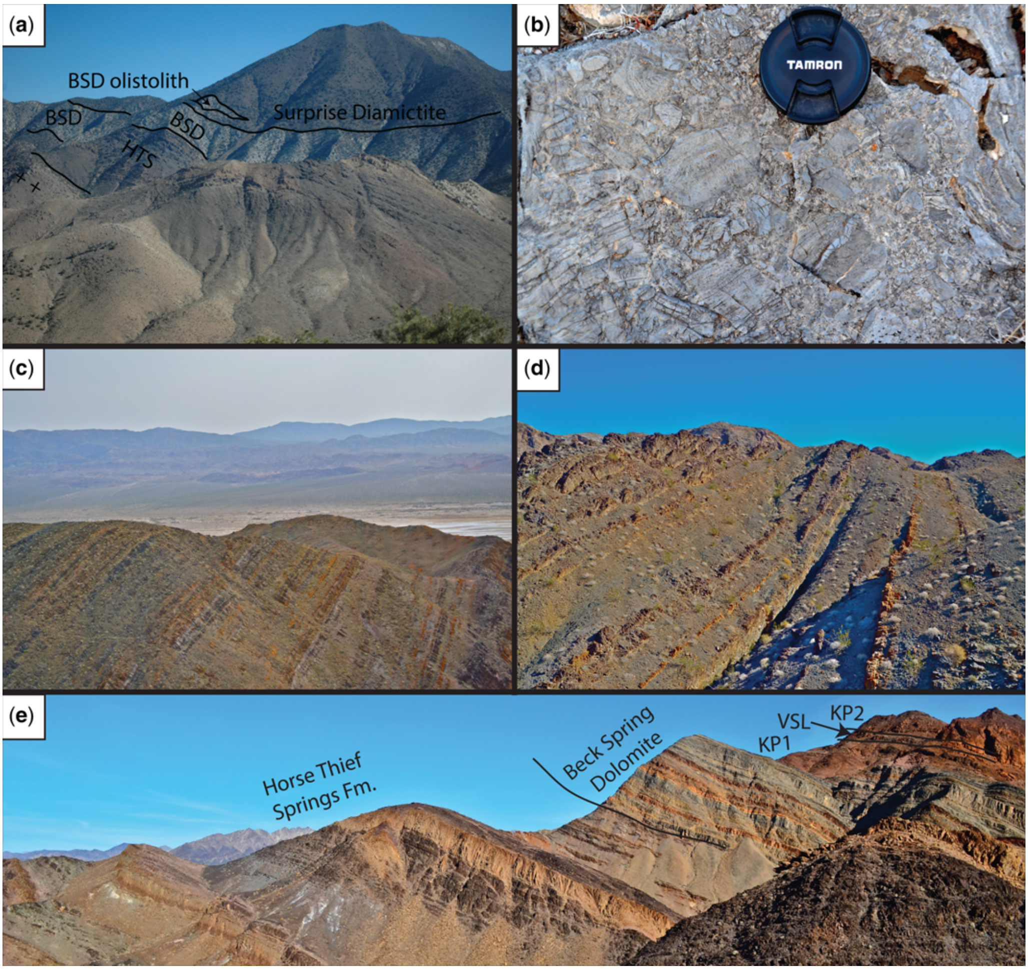

Fig. 6. Pahrump Group photos. Locations of photos in the Kingston Range, Saddle Peak Hills and Saratoga Springs are marked with white triangles in Figures 3 and 4. (**a**) Measured section of Beck Spring Dolomite at Happy Canyon in the Panamint Mountains. Units outlined and labelled in black. (**b**) Beck Spring Dolostone breccia in KP2 near Jupiter Mine in the Kingston Range. (**c**) Mixed siliciclastic–carbonate parasequences at Saratoga Springs. (**d**) Sandstone to conglomerate parasequences at Silurian Hills. Tan dolostones are at the top of Kupfer's unit 10 (see Fig. 5). (**e**) Measured section of TU2 in west-central Saddle Peak Hills (see Fig. 3 for section location).

that there is a gradual shallowing-up in the section. Approximately 30 m from the top of the Beck Spring Dolomite, there is a gradual transgression in which interbedded pisoid (sometimes called 'giant ooids' in the literature) grainstone (Fig. 7e) and microbialite are succeeded by red fissile shale, high-relief, pseudo-branching stromatolites and bedded black chert. Stromatolitic morphologies such as these have been reported from subtidal, low- to moderate-energy environments (Awramik 1971; Donaldson 1976; Hoffman 1976; Horodyski 1977). Additionally, molar tooth structure (Fig. 7c) and black, oolitic limestone beds are present locally near the top of Beck Spring Dolomite. Sampling this section at higher resolution demonstrated that the 'W-shape' profile exists. Data from this section has the most scatter and $\delta^{13}C$ values are on average 2–3‰ lighter throughout the section than in other sampled sections (Fig. 5), perhaps owing to the fact that it is the least carbonate-buffered section sampled (Banner & Hanson 1990). No evidence for exposure is present in the top *c.* 30 m of this section.

The section on the western flank of the Saddle Peak Hills is 110 m thick, significantly thinner than the section measured in Saratoga Springs (Figs 2 & 7e). This change in thickness could be in part due to the placement of the basal contact of

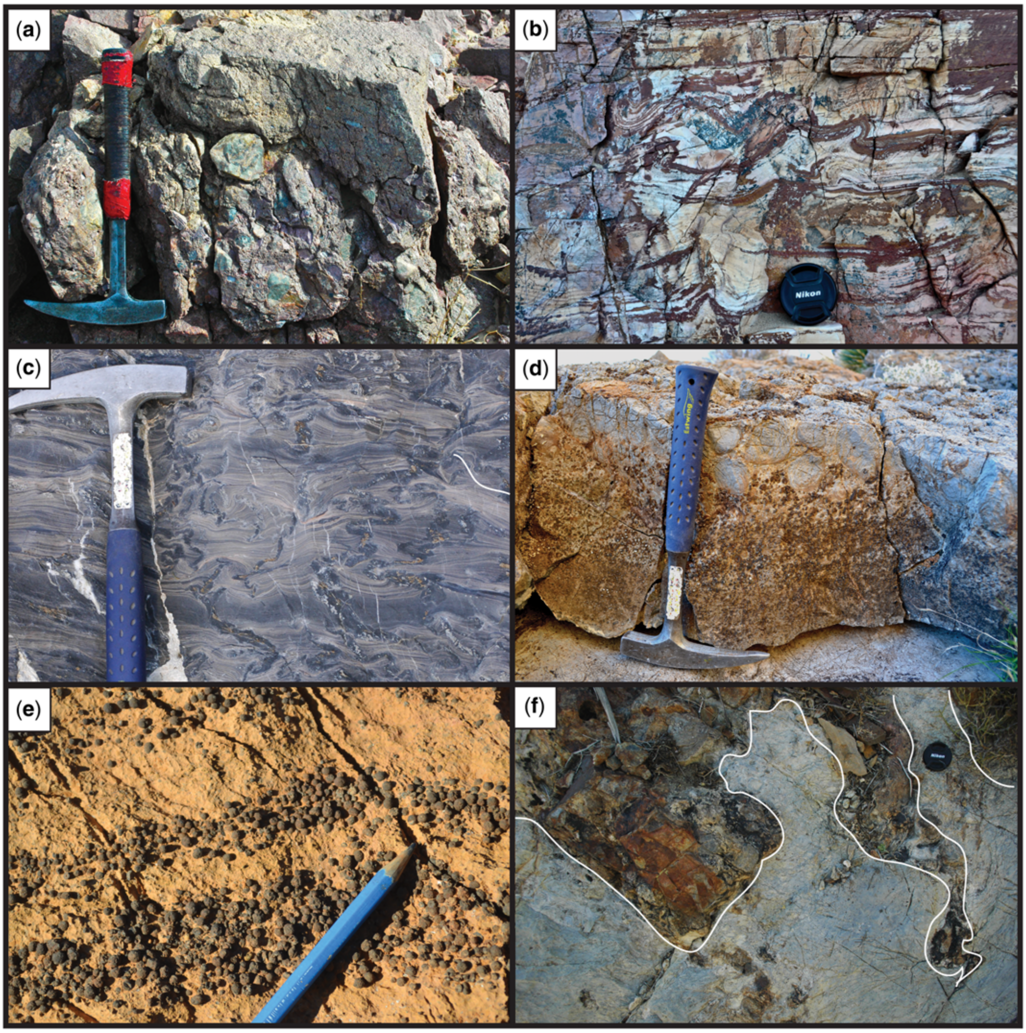

Fig. 7. Sedimentary features of the Beck Spring Dolomite. Locations of photos in the Kingston Range, Saddle Peak Hills, and Saratoga Springs are marked with white triangles in Figures 3 and 4. (**a**) Quartz pebble to cobble conglomerate in the upper part of the Beck Spring Dolomite in west-central Saddle Peak Hills. (**b**) Soft sediment deformation in KP1 in southern Saddle Peak Hills. (**c**) Molar tooth structure in top of the Beck Spring Dolomite at Saratoga Springs. Photograph taken north of measured section. (**d**) Oncoids at the top of the Beck Spring Dolomite sampled from the fault block in western Beck Canyon. (**e**) Giant, partially silicified ooids in the top of the Beck Spring Dolomite in western Saddle Peak Hills. (**f**) White line outlines cross-sectional view of Beck Spring Dolomite sand grykes that are in-filled with the overlying Surprise diamictite in Surprise Canyon, Panamint Mountains.

the Beck Spring Dolomite in what is clearly a gradational contact. However, even by invoking facies change between the two sections, there still must be a significant change in thickness. Aside from the notable change in thickness between the two sections, the sedimentology is similar. Metre-scale mixed siliciclastic–carbonate parasequences with microbial fabrics comprise the base of the section. There is evidence for subaerial exposure in the middle of the section, and the top is composed of re-sedimented dolostone and pisolite. However, owing to small-scale faulting, diagenetic overprinting and sandblasting from nearby sand dunes, the pisoids are variably preserved.

From north to south along the western flank of the Saddle Peak Hills, the Beck Spring Dolomite grades from a *c.* 100 m blue-grey massive dolomite with few siliciclastic interbeds to interbedded dolomite and siliciclastics in well-developed *c.* 1–10 m parasequences. The sandstone and conglomerate beds in this section preserve similar sedimentary features to those in Saratoga Springs. The coarse sandstone beds preserve flat laminations and with bed geometries that vary from quasi-tabular to lensatic. Approximately 3.5 km SE of the measured section in Saddle Peak Hills, just south of where the Virgin Spring Limestone rests unconformably on the Crystal Spring Formation (Fig. 3), the Beck Spring Dolomite is siliciclastic-poor with the exception of two or three very poorly sorted pebble to cobble quartz conglomerates with subrounded clasts of up to 10 cm in diameter near the top of the unit (Fig. 7a). The number of these conglomeratic beds is uncertain owing to fault repetitions.

The section at Beck Canyon is *c.* 290 m thick. We place the basal contact at the orange and black dolostone marker beds that are also present in other sections. Aside from the transition beds at the base and top of the unit, the Beck Spring Dolomite here is almost entirely dolostone that alternates between finely laminated grainstone, microbialaminite, stromatolite and stromatactis. The base has abundant bedded and nodular chert, occasionally with silicified pisoids. Sedimentary breccias are present in the lower–middle part of the section, but are not as abundant as they are in the Alexander Hills (Fig. 5). Like almost all the other sections, ooids and pisoids were found in the middle and top of the section here. Beautifully preserved ooids, pisoids and oncoids are preserved in the upper 10 m of the section in the fault block in the west part of Beck Canyon (Fig. 7d). In this section and the Black Mountain section, more carbonate is preserved at the top of the Beck Spring Dolomite, recording a return to positive values of *c.* +2‰ after the negative $\delta^{13}C$ excursion. In these two sections, the oncolite bed correlates with the basal part of KP1 in other sections. This oncolite bed is the source of the fossiliferous oncolite olistoliths in the Kingston Peak Formation in the Kingston Range (Macdonald *et al.* 2013*a*).

Further to the east, revised mapping shows that the sedimentary Beck breccia, which was previously included in measured sections of the Beck Spring Dolomite near the Jupiter and Snow White mines (Harwood & Sumner 2011), is actually re-deposited Beck Spring Dolomite at the base of KP2 (Fig. 4). Laterally the base of KP2 transitions from Beck Spring Dolomite breccia into a massive diamictite with a mixture of clasts from many of the underlying units. Additionally, in a few gullies near Snow White Mine, there are small outcrops of mixed lithology KP2 glaciogenic facies that underlie the KP2 Beck breccia, confirming that the Beck breccia was deposited during Kingston Peak time rather than as debris infilling palaeokarst caves during Beck Spring time. The heavily silicified horizon beneath the megabreccia is mapped as the basal Kingston Peak unconformity (Fig. 4).

Further north in the SW Black Mountains, the Beck Spring Dolomite is *c.* 295 m of predominantly dolostone. The lower portion of this section is dominated by resedimented dolostone and intraclastic carbonate chip debris flows. There are a few metre-scale beds of intraclastic dolomite breccia composed of pebble- to cobble-sized angular, planar-laminated and stromatolite clasts. There are several beds of pisolites in the middle of the section, and the upper part of the section is dominated by microbialaminite, stromatolite and well-preserved stromatactis. One unusual feature of this section is that there is a 19 m-thick fine-grained sandstone marker bed 30 m below the top contact with KP1. The top 30 m of the section is interbedded shale, silt, bedded chert, partially silicified microbialaminite and conical stromatolites reminiscent of *Conophyton*. Similar to the section in Beck Canyon, oncolites are present in the top bed of the Beck Spring Dolomite here. The contact with KP1 is gradational, and the basal few metres of KP1 contain centimetre-scale silty dolostone beds. Just north of this measured section, the upper *c.* 50 m of the Beck Spring Dolomite is absent, and instead, a thick sedimentary breccia of resedimented dolostone sits on the upper–middle portion of the Beck Spring Dolomite. The nature of the basal and top contacts was not clear owing to fault complications. The $\delta^{13}C$ values at the base of the section are +4 to +6‰, and these positive values persist for *c.* 200 m. There is a negative excursion to −2‰ just below the sandstone marker bed. In the top 30 m of section, there is a return to positive values of +1 to +2‰. Thin tan dolostone beds in the basal *c.* 5 m of KP1 show a steady decrease in $\delta^{13}C$ values.

The section at Happy Canyon in the Panamint Mountains (Fig. 6a) is *c.* 180 m thick. The Beck Spring Dolomite here contains a strong foliation and is pervasively recrystallized. Here, the base of the section is defined as the base of the massive, light grey, resedimented dolostone. Below the Beck Spring Dolomite is a pink, quartz-rich, pebble conglomerate, and it is unclear if this contact is conformable or faulted. The lower to middle part of the section consists predominantly of light grey dolomite grainstone interbedded with local pisoid intervals, some of which are heavily silicified. The middle to upper part of the section is dominated by intraclastic dolostone debris flows and sedimentary breccias with angular clasts of black and white finely laminated dolostone that pinch out laterally over tens of metres. In places, there are microbialaminites and clasts of microbialaminites. Here, the top contact with the Surprise diamictite, which is thought to be correlative with KP3 in southern Death Valley (Prave 1999; Petterson *et al.* 2011; Macdonald *et al.* 2013*a*), is erosive and a kilometre-sized olistolith of the Beck Spring Dolomite is present a few metres above that contact (Fig. 6a). North of this section in Surprise Canyon, the top contact of the Beck Spring Dolomite is marked by sand grykes that are in-filled with Surprise diamictite (Fig. 7f). This is the only locality at which we observed an unconformable karstic surface at the top of the Beck Spring Dolomite, and this karsting has a different age and intensity than the microkarst features that are present throughout the lower to middle Beck Spring Dolomite. Despite the recrystallization of the Happy Canyon section, the $\delta^{13}C$ values are remarkably similar to those in other sections. The $\delta^{13}C$ values at the base of the section rise from *c.* +1.5 to *c.* +4.5‰. In the middle of the section there is a decrease back to *c.* +1.5‰ followed by a gradual rise to *c.* +4.5‰, similar to the 'W-shape' profile that is seen in middle to upper parts of other sections. At the top of the section, there is a negative excursion to *c.* +0.5‰.

Owing to large regional lateral facies changes, it is difficult to definitively identify the Beck Spring Dolomite at the Silurian Hills section. Kupfer's units 11 and 12 (Fig. 5) comprise siliciclastic-dominated, 1–10 m-thick parasequences (Fig. 6d). This interval is 210 m thick and marked by alternating beds of siltstone, sandstone and pebble to cobble conglomerate, similar in thickness to the parasequences in the Beck Spring Dolomite at Saratoga Springs (Fig. 6c). Near the top of the section, the parasequences are mixed siliciclastic and limestone. The top is marked by a 5 m-thick limestone unit containing molar tooth structure (top of Kupfer's unit 12). In Kupfer's units 10 and 11, the $\delta^{13}C$ values range between *c.* −6 and −2‰. At the top of the section, in Kupfer's unit 12, the $\delta^{13}C$ values are more positive, reaching values of *c.* +6.5‰. Kupfer's units 10–12 are correlative with either the Beck Spring Dolomite or the Virgin Spring Limestone. Carbon isotope values from unit 12 and its stratigraphic position directly below massive glacial deposits are very similar (between +1 and +6‰) to that of the Virgin Spring Limestone (Fig. 5).

KP1. KP1 is a fine-grained siliciclastic interval that gradationally overlies the Beck Spring Dolomite. It is 0–200 m thick and occasionally contains centimetre-thick dolostone beds and nodules in the basal part of the unit. KP1 consists predominantly of 1–10 cm-thick beds of siltstone to fine-grained sandstone with minor nodules of finely crystalline dolomite. Sandstone beds are characterized by millimetre-scale, planar parallel laminations, and locally display normal grading. Slump folding and soft sediment deformation in KP1 is pervasive in the SW exposures of the Saddle Peak Hills (Fig. 7b).

In the Panamint Mountains, KP1 is likely equivalent to part of the Limekiln Spring Member of the Kingston Peak Formation (Mrofka 2010); however, in the Happy Canyon section, it is erosively cut out by the Surprise diamictite. In Alexander Hills and Beck Canyon, the top of KP1 is also truncated or absent; the variable thickness is a result of truncation along the unconformable base of TU3, or the base of the Virgin Spring Limestone, and active faulting at the time of deposition of KP1. In the SW Black Mountains, KP1 is *c.* 65 m thick. However, just north of the section, KP1 and the top of the Beck Spring Dolomite are cut out and overlain by a sedimentary breccia composed entirely of clasts of the Beck Spring Dolomite. Further to the NE, at Rhoades Wash, the Virgin Spring Limestone sits unconformably on basement, with a thin sandstone at the basal contact.

Detrital zircon geochronology

Normal probability plots for 15 detrital zircon samples are plotted with a generalized geological map of the southern Mojave crustal province in Figure 8. Samples from the Horse Thief Springs Formation yielded broad peaks at *c.* 1780, 1550, 1450 and 1200 Ma with a minor Archaean peak. Of the 540 grains from the five samples from the Horse Thief Springs Formation that were analysed, there were no grains from the *c.* 780 Ma population that were found by Mahon *et al.* (2014*b*). The two samples from the measured section at Silurian Hills show very similar age distributions to other TU2 samples.

Horse Thief Springs, Beck Spring Dolomite and KP1 samples show peaks at *c.* 1780, 1450 and 1200 Ma, with a minor *c.* 1650 Ma peak. Many of the separates from these samples contain abundant (*c.* 25%) faceted grains. Between the TU2 and Virgin Spring Limestone samples there is a change from spectra with local Mojave sediment sources to spectra with *c.* 1300 and 1580 Ma age peaks (Fig. 8b), suggesting a change in sediment source. Spectra in the KP2 samples display prominent *c.* 1780 peaks with minor *c.* 1450 and 1200 Ma age peaks while the spectra in the KP3 sample just display broad peaks between 1450 and 1200 Ma.

Discussion

TU2 basin reconstructions

Reconstructing Neoproterozoic palaeogeography in Death Valley is complicated by extensive Phanerozoic faulting. The region experienced Permian to Mesozoic orogenesis and magmatism (Burchfiel

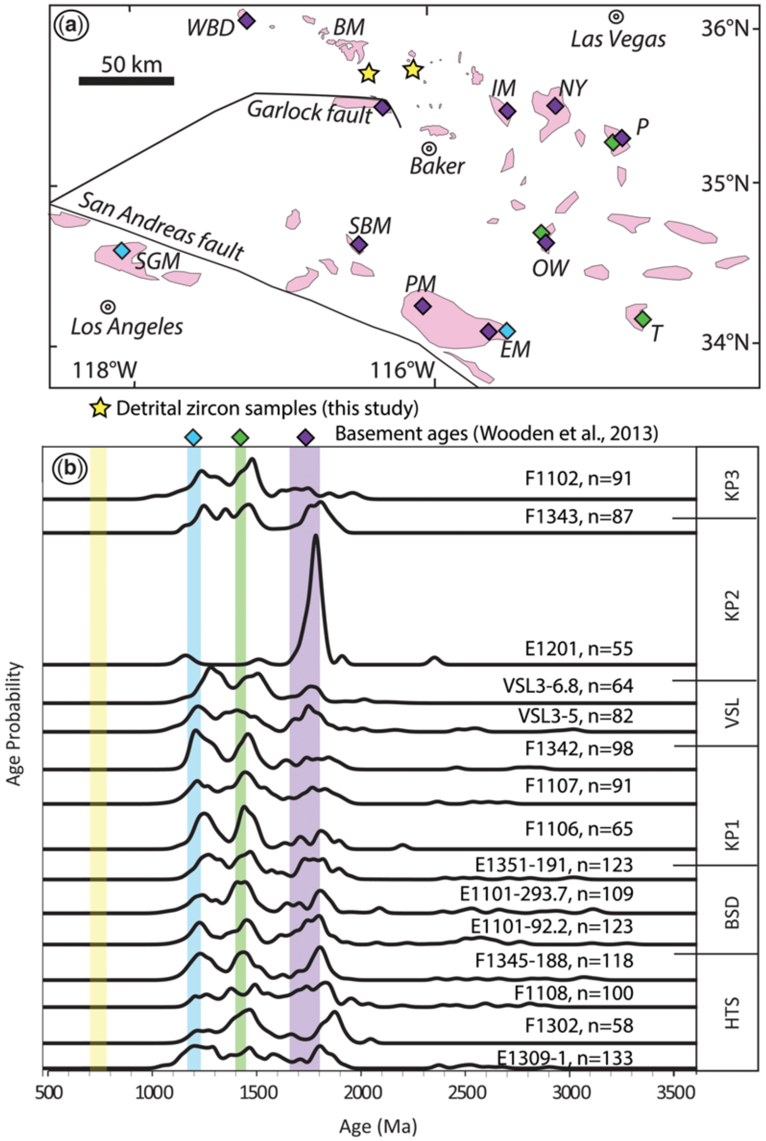

Fig. 8. Detrital zircon geochronology of the Pahrump Group. (**a**) Generalized geological map of the southern Mojave crustal province (adapted from Wooden *et al.* 2013). Blue, green and purple diamonds mark localities sampled by Wooden *et al.* (2013). Yellow stars mark localities of detrital zircon samples presented below. Abbreviations: BM, Black Mountains; EM, Eagle Mountains; IM, Ivanpah Mountains; NY, New York Mountains; OW, Old Woman Mountains; P, Piute Range; PM, Pinto Mountains; SBM, San Bernardino Mountains; SGM, San Gabriel Mountains; T, Turtle Mountains; WBD, World Beater Dome. (**b**) Normal probability plots for 15 detrital zircon samples from SE Death Valley. The specific sections and stratigraphic horizons are indicated in Figure 5. The lower 10 samples are from TU2 and the upper five samples are from TU3. Blue, green and purple shaded bars are basement ages from Wooden *et al.* (2013) and yellow shaded box is the age range for TU2 (Macdonald *et al.* 2013*a*; Mahon *et al.* 2014*b*).

et al. 1970, 1992; Wright *et al.* 1976; Wernicke *et al.* 1988; Snow *et al.* 1991; Snow & Wernicke 2000) with associated felsic and mafic intrusions (Fleck 1970; Wright *et al.* 1991; Calzia *et al.* 2000), followed by right-lateral transtension and the formation of pull-apart basins (Wright 1976; Wright *et al.* 1991; Renik & Christie-Blick 2013). In previous studies, the Mesozoic thrust sheets have been used as piercing points for palinspastic reconstructions (Wernicke *et al.* 1988; Snow & Wernicke 2000; Bergmann *et al.* 2011; Petterson *et al.* 2011); however, much debate remains on the correlation of the thrust sheets (Renik & Christie-Blick 2013). For the NW to SE ordering of the seven measured sections of TU2 (Fig. 5), we also use major Cenozoic and Mesozoic faults, but follow the reconstruction of Renik & Christie-Blick (2013) and Serpa & Pavlis (1996). For our reconstruction of the TU2 basin, the Panamint Mountains are on a different thrust sheet than the stratigraphy of SE Death Valley and do not restore south of the other measured sections in this study. Prave (1999) correlated Kupfner's units 5–12 with the Middle Park–Wildrose succession of the Kingston Peak Formation in the Panamint Range. The structural placement of the Panamint Mountains used in this study is more consistent with the interpretations of Maud (1983) in which the carbonate-dominated Beck Spring Dolomite section in Happy Canyon restores adjacent to the carbonate-dominated sections of the Black Mountains and Alexander Hills rather than in the southern siliciclastic belt in the Silurian Hills.

Depositional model

Horse Thief Springs Formation. The thickest section of the Horse Thief Springs Formation is at the type locality in Beck Canyon. Based on our palinspastic reconstruction and the subsequent arrangement of measured sections from SW to NE (Fig. 5), maximum subsidence occurs in the NE part of the basin. This arrangement of sections, with the siliciclastic-dominated sections in the SW and the carbonate-dominated sections in the NE, is consistent with palaeoflow measurements that suggest that the sediment source was primarily from the south and the shoreline had a NW–SE orientation (Maud 1979). Importantly, between basal TU0 (Macdonald *et al.* 2013*a*; TU1 is assigned to early Neoproterozoic strata from NW Laurentia, but is not present in Death Valley) and TU2, palaeoflow measurements record a marked changed in being derived from the north and east to being derived from the SSW (Maud 1979, 1983; Roberts 1982). These changes in sediment transport direction have been long recognized and were used as a line of evidence in support of the aulacogen model (Roberts 1982). Considering that the duration of the unconformity between TU0 and TU2 is *c.* 200–300 myr (Mahon *et al.* 2014*b*), an alternative model is that TU0 strata formed on a south- and west-facing open margin whereas deposition of TU2 strata marks the onset of a broadly NNE-facing basin bounded by an upland to the south of Death Valley.

Beck Spring Dolomite. Thicknesses and facies patterns of the Beck Spring Dolomite are similar to those of the Horse Thief Springs Formation; the shallower-water facies and more siliciclastic-dominated sections are in the SW and the carbonate-dominated sections are in the NE. We interpret this facies architecture to reflect depositional environments in which a carbonate platform fringed an uplifted land surface to the SW (Fig. 9a).

The siliciclastic-rich facies of the Beck Spring Dolomite in Saratoga Springs and the Saddle Peak Hills contain sedimentary features that are characteristic of coarse-braided fluvial deposits. We interpret the Silurian Hills section, the most southern section measured in this study, as being deposited closer to a southern upland, on the interface between an alluvial apron and coarse fluvial facies (Bull 1972; Blair & McPherson 1994). The base, top and thickness of the Beck Spring Dolomite at this locality are difficult to identify owing to the significant lateral facies change between here and Saratoga Springs. The recrystallized limestone at the top of our measured section (Kupfer's unit 12) looks similar sedimentologically to the Beck Spring Dolomite, but the $\delta^{13}C$ data is more similar to that of the Virgin Spring Limestone (Fig. 5). However, the details of this correlation do not compromise the depositional model.

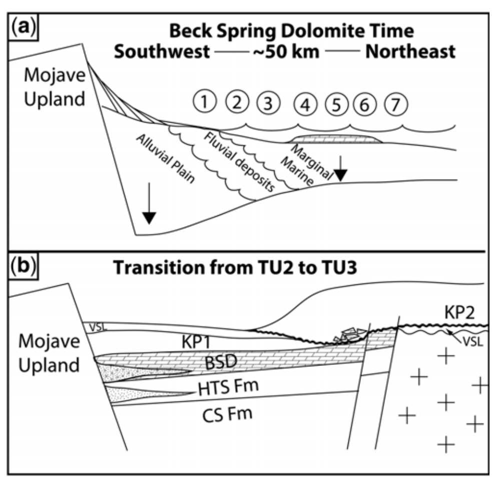

Fig. 9. Schematic depositional and tectonic models for TU2. (**a**) Model for the Beck Spring Dolomite. The circled numbers refer to the general locations of the measured sections in Figure 5 along a simplified SW–NE transect of the basin. (**b**) Tectonic model for the switch in basin polarity that occurs between TU2 and TU3. Unit KP1 and the Virgin Spring Limestone record this transition as a basin-bounding fault emerges. The basin switches from NE-facing to SW-facing across the TU2–TU3 boundary. The thick black line at the base of KP2 is an erosive unconformity.

Overall, our interpretation of the depositional environment of the Beck Springs differs from previous workers who suggested that this unit was deposited on a stable, shallow marine platform in a subtidal to intertidal environment. Instead, we suggest that accommodation space was created quickly in the basin, by either thinning or loading of the crust, while calcifying microbes competed against sediment influx to rapidly fill the space.

KP1. Based on our observations, we suggest that KP1 is part of the transgression that is recorded in the upper part of the Beck Spring Dolomite and was deposited on a more distal prodelta. The influx of siliciclastics that swamps the underlying carbonate platform during this transgression could be the result of either lateral migration of a delta front or the emergence of a basin-bounding fault. Given that there is evidence of syn-sedimentary faulting in TU2 (Mahon 2012; Macdonald *et al.* 2013*a*), we suggest that the siltstone and fine-grained sandstone of KP1 were deposited very quickly with the development of a new basin-bounding fault.

The interpretation that KP1 was deposited during a period of major faulting is consistent with the pervasive slump folding in the Saddle Peak Hills (Fig. 7b) and the stratigraphic relationships of KP1, the Virgin Spring Limestone and the Beck breccia in the Black Mountains. We suggest that the rapid influx of fine sediments during KP1 time marks the onset of basin reorganization (Fig. 9b).

Basin forming mechanisms

The Meso- and Neoproterozoic Pahrump Group through the Ediacaran Johnnie Formation preserve four discrete basin-forming events that record the tectonic and sedimentological history of Death Valley, a promontory on SW Laurentia. Previous tectonic models have suggested that TU2 to TU5 formed in a long-lived rift basin prior to passive margin development in the Cambrian (Yonkee *et al.* 2014 and references cited therein). However, TU2 was deposited more than 200 myr before the rift to drift transition in lower Cambrian strata (Armin & Mayer 1983; Bond *et al.* 1985). Thus, TU2 could not have been deposited by rifting of the proximal western margin. Instead, a model for formation of the ChUMP basin must account for not only local, syn-sedimentary faulting, but also low stretching factors necessary to delay thermal subsidence. TU2 could have been accommodated by transtension, foreland flexure or far-field stresses, including rifting of a more distal margin or extension related to the emplacement of large igneous provinces (LIPs) within Laurentia.

We are not the first to question the protracted rift model. In the eastern Kingston Range, Walker *et al.* (1986) documented Neoproterozoic folding and faulting in the Crystal Spring Formation, Beck Spring Dolomite and the lower part of the Kingston Peak Formation that is overlain by relatively undeformed conglomerate, and questioned tectonic models that invoked simple, protracted rifting. However, some of the thrust faults of Walker *et al.* (1986) are on the margins of olistolith blocks of the Beck Spring Dolomite that were emplaced during syn-Kingston Peak Formation normal faulting (Macdonald *et al.* 2013*a*). In our revised mapping of Kingston Range (Fig. 3), we confirm the presence of folding in the Horse Thief Springs Formation and the Beck Spring Dolomite in western Beck Canyon, but it is unclear if the deformation is Mesozoic in age (Calzia *et al.* 2000) and localized along lithological boundaries in these formations. Folding of TU0 and TU2 on both the metre- and kilometre-scale was also documented in western Saddle Peak Hills (Macdonald *et al.* 2013*a*), but there, it is also unclear if these compressional structures and fabrics formed as a result of Neoproterozoic tectonism or during Mesozoic folding beneath a roof detachment.

Interestingly, deformation of a Neoproterozoic age has been described along a narrow belt in NW Canada, referred to as the Corn Creek Orogeny (Eisbacher 1981; Thorkelson 2000). These structures include dextral shearing and NW-vergent folding and thrusting of *c.* 800 Ma strata of the Mackenzie Mountains Supergroup that are sealed by the *c.* 650 Ma Mt Profeit Dolostone (Macdonald *et al.* 2013*b*). To the east in the Mackenzie Mountains, the Coates Lake Group, which is in part coeval with the Beck Spring Dolomite (Macdonald *et al.* 2013*a*), was interpreted to have formed in a series of dextral strike-slip basins (Eisbacher 1981). These features suggest the Coates Lake Group, equivalent Callison Lake dolostone and the Corn Creek structures formed during dextral transtension and transpression. This strike-slip model is also consistent with the Cryogenian kinematics along the western margin of Laurentia proposed by Li *et al.* (2013) from palaeomagnetic reconstructions.

Characteristic features of strike-slip basins include basin asymmetry, rapid, episodic subsidence, abrupt lateral facies changes, local unconformities and large facies changes in coeval basins that formed in the same region (Christie-Blick 1985). These basins also tend to preserve coarse-clastic units in fault-bounded basins (Ingersoll 1988). Additionally, Reading (1980) predicts that strike-slip faults within continental crust often experience alternating periods of extension and compression as slip directions adjust along a fault. The opening and closing of basins along strike-slip faults is thus referred to as the ‘Reading Cycle’. This model could help explain the multiple unconformity-bound, basin-forming events that occur in the Pahrump Group through Ediacaran strata in Death Valley, and localized deformation that continues up into the Argenta member of the Kingston Peak Formation (Petterson 2009).

In a foreland model, the northeastward progression of siliciclastic input from the SW would represent a growing orogen to the SW culminating with unconformities at the top of KP1. This model could account for the general basin patterns and the appearance of rare *c.* 780 Ma grains on the margin in TU2 strata (Mahon *et al.* 2014*b*), and is not inconsistent with the transtension/transpression model described above. However, more work is necessary to determine if folds in TU2 are pre-Sturtian in age.

Rifting of the supercontinent Rodinia started between 850 and 750 Ma and is associated with the emplacement of several LIPs (Li *et al.* 2008). Rifting of a more distal margin of Laurentia, or subsidence related to the emplacement of the *c.* 780 Ma Gunbarrel LIP in Laurentia and Australia and the coeval Kangding LIP in South China (Li *et al.* 2003, 2007; Lin *et al*. 2007; Ernst *et al.* 2008), may also account for local faulting and the narrow basin formation that accommodated deposition of TU2. However, importantly, these deposits do not record rifting of the proximal western margin of Laurentia that culminated in the Ediacaran to Cambrian passive margin, but instead reflect a distinct and separate tectonothermal event.

Carbon isotope chemostratigraphy and Laurentian correlations

Our data include the first high-resolution $\delta^{13}C$ curve for the Horse Thief Springs Formation. If the $\delta^{13}C$ values presented here reflect the carbon isotopic composition of dissolved inorganic carbon in seawater, then our data show multiple previously undocumented negative carbon isotope excursions between *c.* 780 and 730 Ma. To test the possibility that these values reflect a global signature, they should be reproducible in other correlative Laurentian basins. Alternatively, if the base of TU2 is slightly older than LA-ICPMS detrital zircon ages suggest (Mahon *et al.* 2014*b*), the Horse Thief Springs Formation could be correlative with the Bitter Springs Stage, which has been constrained to between *c.* 811 and 780 Ma (Macdonald *et al.* 2010). This correlation could be tested with additional geochemical analyses that would provide greater age precision on detrital zircons from the base of the Horse Thief Springs Formation.

The $\delta^{13}C$ values of the Beck Spring Dolomite refine correlations within the TU2 basin. The slight downturn in negative $\delta^{13}C$ values in the middle of the ‘W-shape’ profile is a marker of synchronicity that is documented across the basin. Similarly, the negative excursion at the top of the Beck Springs Dolomite is another synchronous marker. Values from the top 5–20 m of the Beck Canyon, Alexander Hills and Black Mountains sections return to positive $\delta^{13}C$ values, demonstrating diachronous deposition of carbonate across the basin. Coupled with remarkable similarity to data from the Callison Lake dolostone (Fig. 10), we suggest that the anomaly at the top of the Beck Spring Dolomite is global and correlative with the *c.* 735 Ma Islay anomaly (Hoffman *et al.* 2012; Strauss *et al.* 2014).

It is also possible that the $\delta^{13}C$ values from TU2 may not represent ancient seawater composition, but rather some local sedimentary processes including authigenic precipitation or post-depositional alteration. However, the isotope excursions appear to be inconsistent with an explanation that invokes surface exposure and alteration through interaction with terrestrial soils (Knauth & Kennedy 2009). There is abundant evidence for exposure in the Horse Thief Springs Formation, but there is no systematic way in which the exposure surfaces correlate with the negative $\delta^{13}C$ values. In fact, some of the carbonates that show evidence for exposure have positive $\delta^{13}C$ values of up to +5‰. In addition, the $\delta^{13}C$ excursions in the Horse Thief Springs Formation are continuous and do not display much variability, a feature that would be expected if the negative excursion was a result of penetration of depleted fluids from terrestrial soils into the underlying carbonate.

Our evidence that the negative isotope excursion at the top of the Beck Spring Dolomite is not related to surface exposure and alteration through terrestrial soils is geological and sedimentological in nature. Our geological mapping of the Beck Spring Dolomite shows that the ‘palaeokarst caves’ that have been reported from the top of the Beck Spring Dolomite in the Kingston Range were formed during Kingston Peak time, not Beck Spring Dolomite time. Additionally, in several of our measured sections, we demonstrate that the $\delta^{13}C$ excursion at the top of the unit is not associated with karsting or exposure but rather a transgression. These are significant results because they demonstrate that this anomaly can no longer be used as evidence for Neoproterozoic greening of land (Knauth & Kennedy 2009).

TU2 has been correlated with the Chuar Group in Arizona, the Uinta Mountain Group in Utah, and the Coates Lake Group and Callison Lake dolostone of NW Canada (Dehler *et al.* 2010; Macdonald *et al.* 2010, 2013*a*; Strauss *et al.* 2014). All five of these basins share similar features and age constrains; however, given that we do not yet understand how to interpret the $\delta^{13}C$ values for the units in TU2, we do not advocate for member- and formation-specific

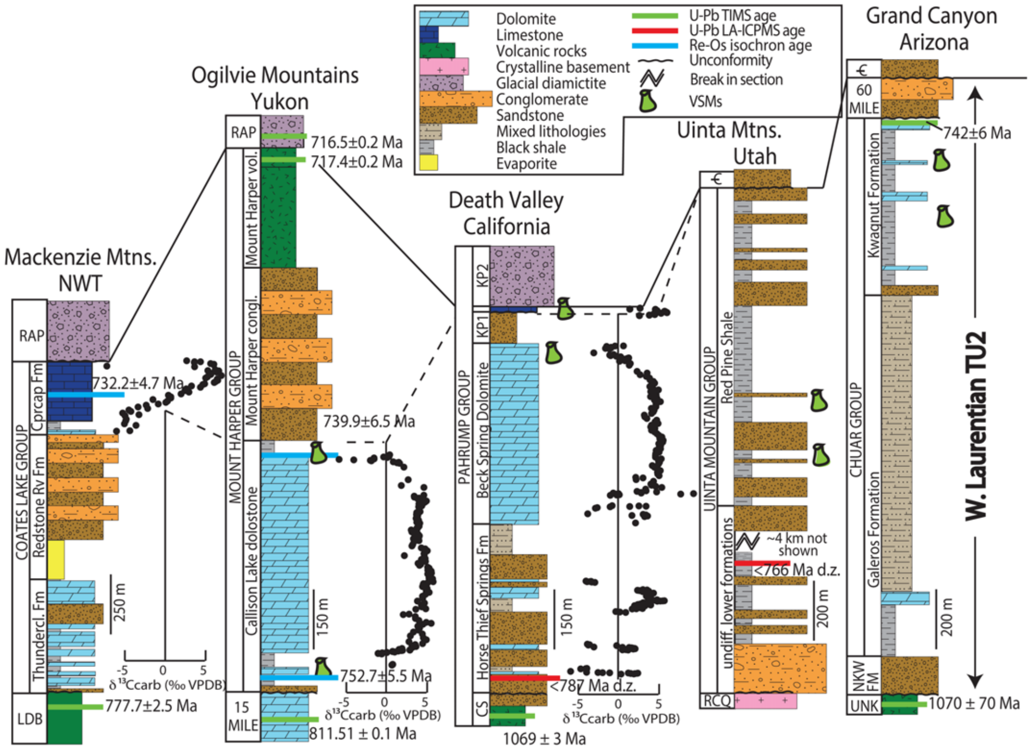

Fig. 10. Refined regional correlations for successions from western US and NW Canada that are generally coeval with TU2 strata in Death Valley. Detrital zircons at the base of the Horse Thief Springs Formation have been dated using laser ablation–inductively coupled plasma mass spectrometry (LA-ICPMS) at *c.* 780 Ma (Mahon *et al.* 2014*b*), providing a maximum age constraint for TU2. Ages at the base of KP2 are from correlation to NW Canada (Macdonald *et al.* 2010, 2013*a*). Age constraints on the Chuar Group include a 742 ± 6 Ma U–Pb zircon age from an ash (Karlstrom *et al.* 2000) at the top of the Kwagunt Formation. The shale at the top of the Callison Lake dolostone has a Re–Os age of 739.9 ± 6.5, providing a date for the Islay excursion (Strauss *et al.* 2014). Additionally, the basal Callison Lake dolostone has a Re–Os age of 752.7 ± 5.5 Ma (Rooney *et al.* 2015). A Re–Os age of 732.2 ± 4.7 Ma is from the organic-rich limestone of the Coppercap Formation of the Coates Lake Group (Rooney *et al.* 2014). VSMs have been identified in the upper Beck Spring Dolomite and Virgin Spring Limestone (Licari 1978; Macdonald *et al.* 2013*a*), the Red Pine Shale (Vidal & Ford 1985), the Kwagunt Formation (Dehler *et al.* 2007) and the Callison Lake dolostone (Strauss *et al.* 2014). Carbonate $\delta^{13}C$ values are plotted for carbonate-rich successions (Macdonald *et al.* 2010, 2013*a*; Rooney *et al.* 2014). This correlation emphasizes a broader correlation of coeval basins along western Laurentia rather than member- and formation-specific ones.

correlations between TU2 and these other basins. We instead emphasize broader correlations between tectonostratigraphic units (Fig. 10). Researchers working on these five basins should continue to look for $\delta^{13}C$ curves similar to those from the Horse Thief Springs Formation and to use geochronology to refine the ages of different members and formations that are part of these basins.

Detrital zircon provenance

Grenville-aged detrital zircons in the Neoproterozoic basins of northern and western Laurentia are commonly interpreted to be sourced from eastern Laurentia via transcontinental rivers (Rainbird *et al.* 1992, 1997; Dehler *et al.* 2010). However, an alternative interpretation is that grains from at least some of these basins were sourced from the more proximal southern extension of the Grenville Province (Anderson & Morrison 1992; Bickford & Anderson 1993). Granites dated at *c.* 1220 Ma are present in the San Gabriel Mountains in SE California (Ekstrom *et al.* 1994; Barth *et al.* 1995, 2001) and New Mexico, Arizona and Chihuahua host granites that are *c.* 1070 Ma (Stewart *et al.* 2001; Rämö *et al.* 2003; Iriondo *et al.* 2004). Neoproterozoic detrital zircon samples from Death Valley offer evidence for a southern, more local sedimentary source.

Sandstone in the Horse Thief Springs Formation contain zircons derived locally from the

Mojave province (1780–1660, 1430–1400, and 1210–1180 Ma; Wooden *et al.* 2013), but also contain grains with ages between *c.* 1950–1800 and 1650–1450 Ma (Fig. 8a, b) that do not have a local basement source. One possibility is that these grains are sourced from reworked Crystal Spring Formation, although the limited detrital zircon data from the Crystal Spring Formation do not yield these ages (Mahon *et al.* 2014*b*). Another possibility is that these grains are sourced from the Yavapai and Mazatzal crustal provinces (Karlstrom & Humphreys 1998; Duebendorfer *et al.* 2001; Cox *et al.* 2002; Rämö *et al.* 2003; Iriondo *et al.* 2004; Amato *et al.* 2008). A third possibility is that an unknown source lay south or west of Laurentia during the Neoproterozoic. Many sandstone beds in the Horse Thief Springs Formation are texturally and compositionally mature, and palaeoflow measurements indicate provenance from the SW (Maud 1979, 1983; Roberts 1982). A source that is consistent with these sedimentological observations is the Gawler Craton of Australia, which includes the *c.* 1850 Ma Donington Suite and the *c.* 1590–1570 Ma Gawler Range Volcanics (Fanning *et al.* 1988; Blissett *et al.* 1993; Peucat *et al.* 2002; Reid & Hand 2012).

In the Beck Spring Dolomite, peaks become sharper and more dominated by the local, Mojave province peaks (Fig. 8b). This is consistent with the interpretation that, as this basin was forming, coeval uplift to the south was occurring and limiting more regional sediment influx to the basin; siliciclastic input into the basin during Beck Spring Dolomite time was tectonically derived from local sources. Stratigraphically higher, in KP1 and the Virgin Spring Limestone, the 1780–1660 Ma peak becomes less dominant. The Virgin Spring Limestone samples contain different age peaks than those in the TU2 samples, suggesting sediment input from an additional source (Fig. 8b). This change in detrital zircon age spectra is consistent with basin reorganization occurring between TU2 and TU3 (Fig. 9b).

Again, during Kingston Peak time, syn-sedimentary normal faults were active and local depocentres developed with palaeoflow generally to the south (Mrofka 2010; Petterson *et al.* 2011). This can be seen in the Saddle Peak Hills area (Fig. 3) and in the Kingston Range (Fig. 4), where the stratigraphy expands southward below a sub-Noonday unconformity (Macdonald *et al.* 2013*a*). KP2 sample E1201 displays a sharp peak at 1780 Ma, implying derivation from local basement, an inference supported by the observation that a large proportion of these grains have severe radiation damage, similar to grains described in the vicinity of World Beater Dome (Lanphere 1962). The other KP2 sample, F1342, has three age peaks between 1500 and 1250 Ma in addition to the 1780 Ma peak. The sample from KP3, a medium-grained sandstone within graded beds, lacks the local 1780 Ma peak, but again displays two broad peaks between 1500 and 1250 Ma, similar to samples from the Virgin Spring Limestone (Fig. 8b).

The detrital zircon data of TU2 in Death Valley show important similarities as well as differences from coeval strata of the Chuar Group in Arizona and the Uinta Mountain Group in Utah (Fig. 11). The 10 samples from TU2 in Death Valley are dominated by the Mojave province peaks while the Chuar and Uinta Mountain Groups have additional sedimentary sources from other Laurentian basement. The samples from the Chuar Group also have a significant 1700–1600 Ma peak from the Mazatzal Province and a 1200–1000 Ma peak from the Grenville Province (Gehrels *et al.* 2011). The age profile of samples from the Uinta Mountain Group is very different from the age distributions of TU2 and the Chuar Group. In addition to minor Mojave-aged peaks, it has a significant Archaean peak from the Wyoming and Superior Cratons, an 1800–1700 Ma peak from the Yavapai and Central Plains provinces, and a 1200–1000 Ma peak from the Grenville Province (Rybczynski 2009; Dehler *et al.* 2010). With the exception of rare *c.* 780 Ma grains, all of the detrital grains in TU2 of Death Valley can be accounted for with local sources to the south in the Mojave block, whereas the Chuar and Uinta Mountains groups show a more cosmopolitan Laurentian signature. These data demonstrate that TU2 detritus was sourced locally from the western margin of Laurentia and not from transcontinental rivers.

Implications for Rodinia reconstructions

Different Rodinia reconstructions have placed Australia, Antarctica, Congo, Kalahari, Siberia, South China and Tasmania along the south and west margins of Laurentia during the early Neoproterozoic (McMenamin & McMenamin 1990; Dalziel 1991; Hoffman 1991; Li *et al.* 1995, 1996, 2008; Karlstrom *et al.* 1999; Burrett & Berry 2000; Sears & Price 2000). Detrital zircon geochronology is one tool that can be used to test these proposed ties. However, detrital zircon age profiles from TU2 of Death Valley, the Uinta Mountain Group and the Chuar Group (Fig. 11), three Laurentian basins that are known to be roughly coeval, show how local sedimentary sources can dominate age populations, potentially limiting the usefulness of this tool. Stratigraphic progression of changing sedimentary sources just within TU2 (Fig. 8b) further demonstrates how active tectonism can mute or eliminate some sedimentary sources within a single basin. Nonetheless, detrital zircon spectra from Neoproterozoic sequences on the Congo, Tasmania,

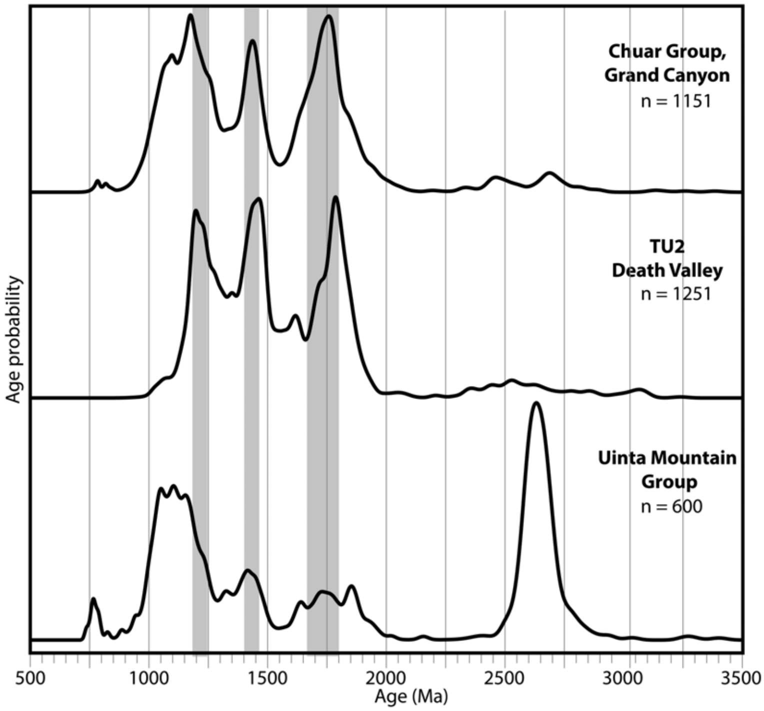

Fig. 11. Detrital zircon age profiles of samples from TU2 in Death Valley, the Chuar Group in Arizona (Gehrels *et al.* 2011) and the Uinta Mountain Group in Utah (Rybczynski 2009; Dehler *et al.* 2010). The ages from Death Valley are from the lower 10 samples in Figure 8b. Probability density plots for the Chuar Group and Uinta Mountain Group show ages that are from a mix of local and continental sources, while the TU2 samples are dominated by ages from very local sources. Shaded grey bars represent Mojave basement ages from Wooden *et al.* (2013).

Australia and the Cathaysia block of South China are generally more similar to the TU2 samples derived primarily from the Mojave block (Fig. 8a, b), whereas those from Neoproterozoic sequences on the Yangtze block of South China, Kalahari and Siberia are distinctly different (Fanning *et al.* 1988; Blissett *et al.* 1993; Li *et al.* 1995, 2002, 2007; Sears & Price 2000; Berry *et al.* 2001; Peucat *et al.* 2002; Black *et al.* 2004; Sears *et al.* 2004; Wang *et al.* 2007; Jacobs *et al.* 2008; Belousova *et al.* 2009; MacLean *et al.* 2009; Goodge *et al.* 2010; Zhao *et al.* 2011; Reid & Hand 2012; Hofmann *et al.* 2014; Konopásek *et al.* 2013).

Additionally, there is no known source for the rare *c.* 790–760 Ma detrital zircons that have been reported from the ChUMP basins (Dehler *et al.* 2010; Mahon *et al.* 2014*b*) and the 742 $\pm$ 6 Ma ash from the top of the Chuar Group (Karlstrom *et al.* 2000). Our study demonstrates that these grains are exceedingly rare, representing less than .01% of grains. Unless grains of this age came from Moine pegmatites in the Dalradian block of eastern Laurentia (Van Breemen *et al.* 1974; Rogers *et al.* 1998) or the Mt Rogers Formation in the southern Appalachians (Aleinikoff *et al.* 1995), and travelled across Laurentia, we should be looking for a source of these young grains to use as a Rodinia piercing point. As discussed above, there is no evidence for transcontinental rivers providing detritus to TU2. Pb–Pb SHRIMP zircon ages from granite on King Island and NW Tasmania yielded ages of 760 $\pm$ 12 and 770 $\pm$ 7 Ma, respectively (Turner *et al.* 1998). It is unclear whether these granites are related to a Neoproterozoic orogenic event (Turner *et al.* 1998) or Neoproterozoic rifting (Berry *et al.* 2008). While speculative, these granites are one possible source for the *c.* 780 Ma grains. Further work is necessary to document the distribution of these grains throughout Laurentia and to refine their age with TIMS. Additionally, 800–720 Ma magmatic ages are common in South China (e.g. Zhou *et al.* 2002). Potential candidates as a source for the 742 $\pm$ 6 Ma Chuar Group ash include the 752–741 Ma Rosh Pinah Formation in the Gariep Belt of the Kalahari Craton of SW Namibia (Frimmel *et al.* 1996) and the 746 $\pm$ 2 Ma Naauwpoort Formation on the Congo Craton of north-central Namibia (Hoffman *et al.* 1996). Basement ages of the Namaqua–Natal Belt of the Kalahari Craton (Eglington 2006) also share similarities with SW Laurentia.

Conclusions

Here we demonstrate that there are large facies changes in the Beck Spring Dolomite and its bounding units over short lateral distances. The new depositional model and detrital zircon analyses presented here extend others' work on the Horse Thief Springs Formation (Maud 1979; 1983; Mahon *et al.* 2014*b*) to suggest that the Beck Spring Dolomite and KP1 also fringed a coeval palaeohigh to the south. During TU2 time, accommodation space was being created quickly in a tectonically active basin, while calcifying microbes competed against sediment influx from the SW to fill the space.

We present new high-resolution carbon isotope chemostratigraphy of the Horse Thief Springs Formation and Beck Spring Dolomite, refining basinal correlations. We demonstrate that the carbon isotope anomaly at the top of the Beck Spring Dolomite is a reproducible feature across the basin and is not associated with karsting or exposure but rather a transgression. Without better age constraints or understanding of the local sedimentary processes affecting carbon isotopes in this basin, we emphasize broader tectonostratigraphic correlations rather than member- and formation-specific chemostratigraphic ones between TU2 and the equivalent strata in the western US (i.e. the ChUMP basins) and NW Canada.

We refine the timing of these three discrete basin-forming events in the Pahrump Group, all of which predate the NW-facing margin during Ediacaran time. In particular, we suggest that TU2 was deposited rapidly around *c.* 735 Ma and did not form during protracted rift-related extensional tectonism of the western margin of Laurentia, but instead records a distinct and separate tectonothermal event.

We thank NAI MIT Astrobiology node for support. We thank T. Prave, C. Burchfiel, C. Dehler and R. Mahon for freely sharing their data and thoughts. We thank G. Eischeid and S. Manley for the use of and assistance in laboratories at Harvard University. We thank S. Lawson, E. Sperling, J. Strauss, S. Pruss, P. Hoffman and R. Petterson for help in the field and helpful discussions. We thank C. Dehler, T. Prave and E. Sperling for constructive criticism and helpful comments on the manuscript. Finally we thank the National Park Service at Death Valley for permitting us to sample within the Park.

References

Aleinikoff, J. N., Zartman, R. E., Walter, M., Rankin, D. W., Lyttle, P. T. & Burton, W. C. 1995. U–Pb ages of metarhyolites of the Catoctin and Mount Rogers formations, Central and Southern Appalachians; evidence for two pulses of Iapetan rifting. *American Journal of Science*, **295**, 428–454.

Amato, J. M., Boullion, A. O., Serna, A. M., Sanders, A. E., Farmer, G. L., Gehrels, G. E. & Wooden, J. L. 2008. Evolution of the Mazatzal province and the timing of the Mazatzal orogeny: insights from U–Pb geochronology and geochemistry of igneous and metasedimentary rocks in southern New Mexico. *Geological Society of America Bulletin*, **120**, 328–346.

Anderson, J. & Morrison, J. 1992. The role of anorogenic granites in the Proterozoic crustal development of North America. *Developments in Precambrian Geology*, **10**, 263–299.

Armin, R. A. & Mayer, L. 1983. Subsidence analysis of the Cordilleran miogeocline: implications for timing of Late Proterozoic rifting and amount of extension. *Geology*, **11**, 702–705.

Awramik, S. M. 1971. Precambrian columnar stromatolite diversity: reflection of metazoan appearance. *Science*, **174**, 825–827.

Banner, J. L. & Hanson, G. N. 1990. Calculation of simultaneous isotopic and trace element variations during water–rock interaction with applications to carbonate diagenesis. *Geochimica et Cosmochimica Acta*, **54**, 3123–3137.

Barth, A. P., Wooden, J., Tosda, R., Morrison, J., Dawson, D. & Hernly, B. 1995. Origin of gneisses in the aureole of the San Gabriel anorthosite complex and implications for the Proterozoic crustal evolution of southern California. *Tectonics*, **14**, 736–752.

Barth, A. P., Wooden, J. L., Coleman, D. S. & Fanning, C. M. 2000. Geochronology of the Proterozoic basement of southwesternmost North America, and the origin and evolution of the Mojave crustal province. *Tectonics*, **19**, 616–629.

Barth, A. P., Wooden, J. L. & Coleman, D. S. 2001. SHRIMP-RG U–Pb Zircon Geochronology of Mesoproterozoic Metamorphism and Plutonism in the Southwesternmost United States. *The Journal of Geology*, **109**, 319–327.

Belousova, E., Reid, A., Griffin, W. L. & O'Reilly, S. Y. 2009. Rejuvenation v. recycling of Archean crust in the Gawler Craton, South Australia: evidence from U–Pb and Hf isotopes in detrital zircon. *Lithos*, **113**, 570–582.

Bergmann, K. D., Zentmyer, R. A. & Fischer, W. W. 2011. The stratigraphic expression of a large negative carbon isotope excursion from the Ediacaran Johnnie Formation, Death Valley. *Precambrian Research*, **188**, 45–56.

Berry, R., Jenner, G., Meffre, S. & Tubrett, M. 2001. A North American provenance for Neoproterozoic to Cambrian sandstones in Tasmania? *Earth and Planetary Science Letters*, **192**, 207–222.

Berry, R. F., Steele, D. A. & Meffre, S. 2008. Proterozoic metamorphism in Tasmania: implications for tectonic reconstructions. *Precambrian Research*, **166**, 387–396.

Bickford, M. & Anderson, J. 1993. Middle Proterozoic magmatism. *Geology of North America*, **2**, 281–292.

Black, L. P., Kamo, S. L., *et al.* 2004. Improved (206)Pb/(238)U microprobe geochronology by the monitoring of a trace-element-related matrix effect; SHRIMP, ID-TIMS, ELA-ICP-MS and oxygen isotope documentation for a series of zircon standards. *Chemical Geology*, **205**, 115–140.

Blair, T. C. & McPherson, J. G. 1994. Alluvial fans and their natural distinction from rivers based on morphology, hydraulic processes, sedimentary processes, and facies assemblages. *Journal of Sedimentary Research*, **64**, 450–489.

Blissett, A., Creaser, R., Daly, S., Flint, R. & Parker, A. 1993. Gawler range volcanics. *The Geology of South Australia*, **1**, 107–124.

Bloeser, B. 1985. Melanocyrillium, a new genus of structurally complex late Proterozoic microfossils from the Kwagunt Formation (Chuar Group), Grand Canyon, Arizona. *Journal of Paleontology*, **59**, 741–765.

Bond, G. C. & Kominz, M. A. 1984. Construction of tectonic subsidence curves for the early Paleozoic miogeocline, southern Canadian Rocky Mountains: implications for subsidence mechanisms, age of breakup, and crustal thinning. *Geological Society of America Bulletin*, **95**, 155–173.

Bond, G. C., Christieblick, N., Kominz, M. A. & Devlin, W. J. 1985. An early Cambrian rift to post-rift transition in the Cordillera of western North-America. *Nature*, **315**, 742–746.

Brehm, C. 2008. *Sedimentology, Stratigraphy, and Organic Geochemistry of the Red Pine Shale, Uinta Mountains, Utah: A prograding Deltaic System in a 'Western Neoproterozoic Seaway'*. MS thesis, Utah State University.

Bull, W. B. 1972. Recognition of alluvial fan deposits in the stratigraphic record. *In*: Rigby, J. K. & Hamblin, W. K. (eds) *Recognition of Ancient Sedimentary Environments*. Society of Economic Paleontologists and Mineralogists, Tulsa, OK, Special Publications, **16**, 63–83.

Burchfiel, B. C., Pelton, P. J. & Sutter, J. 1970. An early Mesozoic deformation belt in south-central Nevada-southeasterrn California. *Geological Society of America Bulletin*, **81**, 211–215.

Burchfiel, B. C., Cowan, D. S. & Davis, G. A. 1992. Tectonic overview of the Cordilleran orogen in the western United States. *In*: Burchfiel, B. C., Lipman, P. W. & Zoback, M. L. (eds) *The Cordilleran Orogen: Conterminous U.S.* The Geology of North America, **G-3**. Geological Society of America, Boulder, CO, 407–479.

Burrett, C. & Berry, R. 2000. Proterozoic Australia–Western United States (AUSWUS) fit between Laurentia and Australia. *Geology*, **28**, 103–106.

Calver, C., Crowley, J., Wingate, M., Evans, D., Raub, T. & Schmitz, M. 2013. Globally synchronous Marinoan deglaciation indicated by U–Pb geochronology of the Cottons Breccia, Tasmania, Australia. *Geology*, **41**, 1127–1130.

Calzia, J. P., Troxel, B. W., Wright, L. A., Burchfiel, B. C., Davis, G. A. & McMackin, M. R. 2000. *Geologic map of the Kingston Range, southern Death Valley, California*, Open-File Report: US Geological Survey, 2 sheets.

Christie-Blick, N. 1985. Deformation and basin formation along strike-slip faults.

Clapham, M. E. & Corsetti, F. A. 2005. Deep valley incision in the terminal Neoproterozoic (Ediacaran) Johnnie Formation, eastern California, USA: tectonically or glacially driven? *Precambrian Research*, **141**, 154–164.

Cloud, P. & Semikhatov, M. 1969. Proterozoic stromatolite zonation. *American Journal of Science*, **267**, 1017–1061.

Cloud, P. E., Licari, G. R., Wright, L. A. & Troxel, B. W. 1969. Proterozoic eucaryotes from Eastern California. *Proceedings of the National Academy of Sciences of the United States of America*, **62**, 623–631.

Condon, D., Zhu, M. Y., Bowring, S., Wang, W., Yang, A. H. & Jin, Y. G. 2005. U–Pb ages from the Neoproterozoic Doushantuo Formation, China. *Science*, **308**, 95–98.

Corsetti, F. A. & Kaufman, A. J. 2003. Stratigraphic investigations of carbon isotope anomalies and Neoproterozoic ice ages in Death Valley, California. *Geological Society of America Bulletin*, **115**, 916–932.

Cox, R., Martin, M. W., Comstock, J. C., Dickerson, L. S., Ekstrom, I. L. & Sammons, J. H. 2002. Sedimentology, stratigraphy, and geochronology of the Proterozoic Mazatzal Group, central Arizona. *Geological Society of America Bulletin*, **114**, 1535–1549.

Dalziel, I. W. D. 1991. Pacific margins of Laurentia and east Antarctica Australia as a conjugate rift pair – evidence and implications for an Eocambrian supercontinent. *Geology*, **19**, 598–601.

Dehler, C. M., Elrick, M., Karlstrom, K. E., Smith, G. A., Crossey, L. J. & Timmons, J. M. 2001. Neoproterozoic Chuar Group (similar to 800–742 Ma), Grand Canyon: a record of cyclic marine deposition during global cooling and supercontinent rifting. *Sedimentary Geology*, **141**, 465–499.

Dehler, C. M., Elrick, M., Bloch, J. D., Crossey, L. J., Karlstrom, K. E. & Des Marais, D. J. 2005. High-resolution delta C-13 stratigraphy of the Chuar Group (*c.* 770–742 Ma), Grand Canyon: implications for mid-Neoproterozoic climate change. *Geological Society of America Bulletin*, **117**, 32–45.

Dehler, C. M., Porter, S. M., De Grey, L. D., Sprinkel, D. A. & Brehm, A. 2007. The Neoproterozoic Uinta Mountain Group revisited: a synthesis of recent work on the Red Pine Shale and undivided clastic strata, northeastern Utah: proterozoic geology of western North America and Siberia. *Society of Sedimentary Geology, Special Publication*, **86**, 151–166.

Dehler, C. M., Fanning, C. M., Link, P. K., Kingsbury, E. M. & Rybczynski, D. 2010. Maximum depositional age and provenance of the Uinta Mountain Group and Big Cottonwood Formation, northern Utah: paleogeography of rifting western Laurentia. *Geological Society of America Bulletin*, **122**, 1686–1699.

Donaldson, J. 1976. Paleoecology of conophyton and associated stromatolites in the Precambrian Dismal Lakes and Rae Groups, Canada. *Developments in Sedimentology*, **20**, 523–534.

Duebendorfer, E. M., Chamberlain, K. R. & Jones, C. S. 2001. Paleoproterozoic tectonic history of the Cerbat Mountains, northwestern Arizona: implications for crustal assembly in the southwestern United States. *Geological Society of America Bulletin*, **113**, 575–590.

Eglington, B. 2006. Evolution of the Namaqua–Natal Belt, southern Africa – a geochronological and isotope geochemical review. *Journal of African Earth Sciences*, **46**, 93–111.

Eisbacher, G. H. 1981. *Sedimentary Tectonics and Glacial Record in the Windermere Supergroup, Mackenzie Mountains, Northwestern Canada*. Geological Survey of Canada, St John's, Newfoundland.

Ekstrom, H., Morrison, J. & Anderson, J. L. 1994. Petrogenetic modeling and stable isotopic evaluation of anorthositic and jotunitic to syenitic magma series in the San Gabriel anorthosite complex, southern California. *Precambrian Research*, **70**, 1–24.

Ernst, R., Wingate, M., Buchan, K. & Li, Z. 2008. Global record of 1600–700 Ma Large Igneous Provinces (LIPs): implications for the reconstruction of the proposed Nuna (Columbia) and Rodinia supercontinents. *Precambrian Research*, **160**, 159–178.

Fanning, C., Flint, R., Parker, A., Ludwig, K. & Blissett, A. 1988. Refined Proterozoic evolution of the Gawler craton, South Australia, through U–Pb zircon geochronology. *Precambrian Research*, **40**, 363–386.

Fedo, C. M. & Cooper, J. D. 2001. Sedimentology and sequence stratigraphy of Neoproterozoic and Cambrian units across a craton-margin hinge zone, southeastern California, and implications for the early evolution of the Cordilleran margin. *Sedimentary Geology*, **141**, 501–522.

Fleck, R. J. 1970. Age and tectonic significance of volcanic rocks, Death Valley area, California. *Geological Society of America Bulletin*, **81**, 2807–2816.

Frimmel, H. E., Klötzli, U. S. & Siegfried, P. R. 1996. New Pb–Pb single zircon age constraints on the timing of Neoproterozoic glaciation and continental break-up in Namibia. *The Journal of Geology*, **104**, 459–469.

Gehrels, G. E., Blakey, R., Karlstrom, K. E., Timmons, J. M., Dickinson, B. & Pecha, M. 2011. Detrital zircon U–Pb geochronology of Paleozoic strata in the Grand Canyon, Arizona. *Lithosphere*, **3**, 183–200.

Goodge, J. W., Fanning, C. M., Brecke, D. M., Licht, K. J. & Palmer, E. F. 2010. Continuation of the Laurentian Grenville province across the Ross Sea margin of East Antarctica. *The Journal of Geology*, **118**, 601–619.

Gutstadt, A. M. 1968. Petrology and depositional environments of the Beck Spring Dolomite (Precambrian), Kingston Range, California. *Journal of Sedimentary Research*, **38**, 1280–1289.

Harwood, C. L. & Sumner, D. Y. 2011. Microbialites of the Neoproterozoic Beck Spring Dolomite, Southern California. *Sedimentology*, **58**, 1648–1673.

Harwood, C. L. & Sumner, D. Y. 2012. Origins of microbial microstructures in the Neoproterozoic Beck Spring Dolomite: variations in microbial community and timing of lithification. *Journal of Sedimentary Research*, **82**, 709–722.

Heaman, L. M. & Grotzinger, J. P. 1992. 1.08 Ga diabase sills in the Pahrump Group, California; implications for development of the Cordilleran Miogeocline. *Geology*, **20**, 637–640.

Hewett, D. 1940. New formation names to be used in the Kingston Range: Ivanpah Quadrangle, California. *Washington Academy of Sciences Journal*, **30**, 239–240.

Hoffman, P. F. 1976. Environmental Diversity of Middle Precambrian Stromatolites. *Developments in Sedimentology*, **20**, 599–611.

Hoffman, P. F. 1991. Did the breakout of Laurentia turn Gondwanaland inside-out? *Science*, **252**, 1409–1412.

Hoffman, P. F., Hawkins, D. P., Isachsen, C. E. & Bowring, S. A. 1996. Precise U–Pb zircon ages for early Damaran magmatism in the Summas Mountains and Welwitschia Inlier, northern Damara belt, Namibia. *Communications of the Geological Survey of Namibia*, **11**, 47–52.

Hoffman, P. F., Halverson, G. P., Domack, E. W., Maloof, A. C., Swanson-Hysell, N. L. & Cox, G. M. 2012. Cryogenian glaciations on the southern tropical paleomargin of Laurentia (NE Svalbard and East Greenland), and a primary origin for the upper Russoya (Islay) carbon isotope excursion. *Precambrian Research*, **206**, 137–158.

Hoffmann, K. H., Condon, D. J., Bowring, S. A. & Crowley, J. L. 2004. U–Pb zircon date from the Neoproterozoic Ghaub Formation, Namibia. *Constraints on Marinoan Glaciation: Geology*, **32**, 817–820.

Hofmann, M., Linnemann, U., Hoffmann, K.-H., Gerdes, A., Eckelmann, K. & Gärtner, A. 2014. The Namuskluft and Dreigratberg sections in southern Namibia (Kalahari Craton, Gariep Belt): a geological history of Neoproterozoic rifting and recycling of cratonic crust during the dispersal of Rodinia until the amalgamation of Gondwana. *International Journal of Earth Sciences*, **103**, 1187–1202.

Horodyski, R. J. 1977. Lyngbya mats at Laguna Mormona, Baja California, Mexico; comparison with Proterozoic stromatolites. *Journal of Sedimentary Research*, **47**, 1305–1320.

Horodyski, R. J. & Knauth, L. P. 1994. Life on land in the Precambrian. *Science*, **263**, 494–498.

Hurtgen, M. T., Arthur, M. A. & Prave, A. R. 2004. The sulfur isotope composition of carbonate-associated sulfate in Mesoproterozoic to Neoproterozoic carbonates from Death Valley, California. Geological Society of America, Boulder, CO, Special Papers, **379**, 177–194.

Ingersoll, R. V. 1988. Tectonics of sedimentary basins. *Geological Society of America Bulletin*, **100**, 1704–1719.

Iriondo, A., Premo, W. R., Martínez-Torres, L. M., Budahn, J. R., Atkinson, W. W., Siems, D. F. & Guarás-González, B. 2004. Isotopic, geochemical, and temporal characterization of Proterozoic basement rocks in the Quitovac region, northwestern Sonora, Mexico: implications for the reconstruction of the southwestern margin of Laurentia. *Geological Society of America Bulletin*, **116**, 154–170.

Jacobs, J., Pisarevsky, S., Thomas, R. J. & Becker, T. 2008. The Kalahari Craton during the assembly and dispersal of Rodinia. *Precambrian Research*, **160**, 142–158.

Jefferson, C. & Parrish, R. 1989. Late Proterozoic stratigraphy, U–Pb zircon ages, and rift tectonics, Mackenzie Mountains, northwestern Canada. *Canadian Journal of Earth Sciences*, **26**, 1784–1801.

Karlstrom, K. E. & Humphreys, E. D. 1998. Persistent influence of Proterozoic accretionary boundaries in the tectonic evolution of southwestern North America Interaction of cratonic grain and mantle modification events. *Rocky Mountain Geology*, **33**, 161–179.

Karlstrom, K. E., Harlan, S. S., Williams, M. L., McLelland, J., Geissman, J. W. & Ahall, K.-I. 1999. Refining Rodinia: geologic evidence for the Australia–western US connection in the Proterozoic. *GSA Today*, **9**, 1–7.

Karlstrom, K. E., Bowring, S. A., *et al.* 2000. Chuar Group of the Grand Canyon: record of breakup of Rodinia, associated change in the global carbon cycle, and ecosystem expansion by 740 Ma. *Geology*, **28**, 619–622.

Kenny, R. & Knauth, L. P. 2001. Stable isotope variations in the Neoproterozoic Beck Spring Dolomite and Mesoproterozoic Mescal Limestone paleokarst: implications for life on land in the Precambrian. *Geological Society of America Bulletin*, **113**, 650–658.

Knauth, L. P. & Kennedy, M. J. 2009. The late Precambrian greening of the Earth. *Nature*, **460**, 728–732.

Konopásek, J., Košler, J., Sláma, J. & Janoušek, V. 2013. *Timing and Sources of Pre-Collisional Neoproterozoic Sedimentation Along the SW Margin of the Congo Craton*. Kaoko Belt, NW Namibia, Gondwana Research.

Kupfer, D. H. 1960. Thrust faulting and chaos structure, Silurian Hills, San Bernardino County, California. *Geological Society of America Bulletin*, **71**, 181–214.

Labotka, T. C., Albee, A. L., Lanphere, M. A. & McDowell, S. D. 1980. Stratigraphy, structure, and metamorphism in the central Panamint Mountains (Telescope-Peak Quandrangle), Death-Valley Area, California – Summary. *Geological Society of America Bulletin*, **91**, 125–129.

Lanphere, M. A. 1962. *I. Geology of the Wildrose area, Panamint Range, California. II. Geochronologic studies in the Death Valley-Mojave Region, California*. PhD, California Institute of Technology.

Li, Z., Zhang, L. & Powell, C. M. 1996. Positions of the East Asian cratons in the Neoproterozoic supercontinent Rodinia. *Australian Journal of Earth Sciences*, **43**, 593–604.

Li, Z.-X., Zhang, L. & Powell, C. M. 1995. South China in Rodinia: part of the missing link between Australia–East Antarctica and Laurentia? *Geology*, **23**, 407–410.

Li, Z.-X., Li, X. H., Zhou, H. & Kinny, P. D. 2002. Grenvillian continental collision in south China: new SHRIMP U–Pb zircon results and implications for the configuration of Rodinia. *Geology*, **30**, 163–166.

Li, Z.-X., Li, X., Kinny, P., Wang, J., Zhang, S. & Zhou, H. 2003. Geochronology of Neoproterozoic syn-rift magmatism in the Yangtze Craton, South China and correlations with other continents: evidence for a mantle superplume that broke up Rodinia. *Precambrian Research*, **122**, 85–109.

Li, Z. X., Wartho, J., Occhipinti, S., Zhang, C. L., Li, X. H., Wang, J. & Bao, C. M. 2007. Early history of the eastern Sibao Orogen (South China) during the assembly of Rodinia: new mica 40Ar-39Ar dating and SHRIMP U–Pb detrital zircon provenance constraints. *Precambrian Research*, **159**, 79–94.

Li, Z.-X., Bogdanova, S., *et al.* 2008. Assembly, configuration, and break-up history of Rodinia: a synthesis. *Precambrian Research*, **160**, 179–210.

Li, Z.-X., Evans, D. A. & Halverson, G. P. 2013. Neoproterozoic glaciations in a revised global palaeogeography from the breakup of Rodinia to the assembly of Gondwanaland. *Sedimentary Geology*, **294**, 219–232.

Licari, G. R. 1978. Biogeology of late Pre-Phanerozoic Beck Spring Dolomite of eastern California. *Journal of Paleontology*, **52**, 767–792.

Lin, G., Li, X. & Li, W. 2007. SHRIMP U–Pb zircon age, geochemistry and Nd–Hf isotope of Neoproterozoic mafic dyke swarms in western Sichuan: petrogenesis and tectonic significance: science in China Series D. *Earth Sciences*, **50**, 1–16.

Link, P. K., Christie-Blick, N., *et al.* 1993. Middle and Late Proterozoic stratified rocks of the western Cordillera, Colorado Plateau, and Basin and Range province. *In*: Reed, J. C., Jr. *et al.* (eds) *Precambrian: Conterminous U.S*. Geological Society of America, Boulder, Colorado, Geology of North America, C-2, 463–596.

Loyd, S. J. & Corsetti, F. A. 2010. The origin of the millimeter-scale lamination in the Neoproterozoic lower Beck Spring Dolomite: implications for widespread, fine-scale, layer-parallel diagenesis in Precambrian carbonates. *Journal of Sedimentary Research*, **80**, 678–687.

Macdonald, F. A., Schmitz, M. D., *et al.* 2010. Calibrating the cryogenian. *Science*, **327**, 1241–1243.

Macdonald, F. A., Prave, A. R., *et al.* 2013*a*. The Laurentian record of Neoproterozoic glaciation, tectonism, and eukaryotic evolution in Death Valley, California. *Geological Society of America Bulletin*, **125**, 1203–1223.

Macdonald, F. A., Strauss, J. V., *et al.* 2013*b*. The stratigraphic relationship between the Shuram carbon isotope excursion, the oxygenation of Neoproterozoic oceans, and the first appearance of the Ediacara biota and bilaterian trace fossils in northwestern Canada. *Chemical Geology*, **362**, 250–272.

MacLean, J., Sears, J., Chamberlain, K., Khudoley, A., Prokopiev, A., Kropachev, A. & Serkina, G. 2009. Detrital zircon geochronologic tests of the SE Siberia–SW Laurentia paleocontinental connection. Stephan Mueller Special Publication Series, **4**, 111–116.

Mahon, R. C. 2012. *Detrital zircon Provenance, Geochronology and Revised stratigraphy of the Mesoproterozoic and Neoproterozoic Pahrump (Super)Group, Death Valley Region, California and Geology of the Saddle Peak Hills 7.5' Quadrangle, San Bernardino County, California*. MS, Idaho State University.

Mahon, R. C., Dehler, C. M., Link, P. K., Karlstrom, K. E. & Gehrels, G. E. 2014*a*. *Detrital Zircon Provenance and Paleogeography of the Pahrump Group and Overlying Strata, Death Valley*. Precambrian Research, California.

Mahon, R. C., Dehler, C. M., Link, P. K., Karlstrom, K. E. & Gehrels, G. E. 2014*b*. Geochronologic and stratigraphic constraints on the Mesoproterozoic and Neoproterozoic Pahrump Group, Death Valley, California: a record of the assembly, stability, and breakup of Rodinia. *Geological Society of America Bulletin*, **126**, 652–664.

Marian, M. L. 1979. *Sedimentology of the Beck Spring Dolomite, eastern Mojave Desert*. MS thesis, University of Southern California.

Marian, M. L. & Osborne, R. H. 1992. Petrology, petrochemistry, and stromatolites of the middle to late Proterozoic Beck Spring Dolomite, eastern Mojave Desert, California. *Canadian Journal of Earth Sciences*, **29**, 2595–2609.

Maud, R. L. 1979. *Stratigraphy and Depositional Environments of the Carbonate-terrigenous Member of the Crystal Spring Formation*. MS thesis, Pennsylvania State University, 177 p.

Maud, R. L. 1983. *Stratigraphy, Petrography and Depositional Environments of the Carbonate-terrigenous Member of the Crystal Spring Formation*. PhD thesis, Pennsylvania State University.

Mbuyi, K. & Prave, A. R. 1993. Unconformities in the mid-late Proterozoic Pahrump Group: stratigraphic evidence from the upper member Crystal Spring Formation. *Proceedings Geological Society of America, Abstracts with Programs*, **25**, 98.

McMenamin, M. A. & McMenamin, D. L. S. 1990. *The Emergence of Animals: The Cambrian Breakthrough*. Columbia University Press, New York.

Miller, J. M. G. 1985. Glacial and syntectonic sedimentation: the upper Proterozoic Kinston Peak Formation, southern Panamint Range, eastern California. *Geological Society of America Bulletin*, **96**, 75–85.

Moores, E. M. 1991. Southwest United-States–East Antarctic (SWEAT) connection – a hypothesis. *Geology*, **19**, 425–428.

Mrofka, D. D. 2010. *Competing Models for the Timing of Cryogenian Glaciation: Evidence from the Kingston Peak Formation, Southeastern California* PhD thesis, University of California, Riverside, CA.

Nelson, C. 1978. Late Precambrian–Early Cambrian stratigraphic and faunal succession of eastern California and the Precambrian–Cambrian boundary. *Geological Magazine*, **115**, 121–126.

Noble, L. F. 1934. Rock formations of Death Valley, California. *Science*, **80**, 173–178.

Petterson, R. 2009. *The Basal Ediacaran Noonday Formation, Eastern California, and Implications for Laurentian Equivalents* PhD thesis, California Institute of Technology, 225 p.

Petterson, R., Prave, A. R., Wernicke, B. P. & Fallick, A. E. 2011. The Neoproterozoic Noonday Formation, Death Valley region, California. *Geological Society of America Bulletin*, **123**, 1317–1336.

Peucat, J., Capdevila, R., Fanning, C., Ménot, R., Pécora, L. & Testut, L. 2002. 1.60 Ga felsic volcanic blocks in the moraines of the Terre Adélie Craton, Antarctica: comparisons with the Gawler Range Volcanics, South Australia. *Australian Journal of Earth Sciences*, **49**, 831–845.

Pierce, D. & Cloud, P. 1979. New microbial fossils from 1.2 billion-year-old rocks of eastern California. *Geomicrobiology Journal*, **1**, 295–309.

Porter, S. M. & Knoll, A. H. 2000. Testate amoebae in the Neoproterozoic Era: evidence from vase-shaped microfossils in the Chuar Group, Grand Canyon. *Paleobiology*, **26**, 360–385.

Prave, A. R. 1999. Two diamictites, two cap carbonates, two delta C-13 excursions, two rifts: the Neoproterozoic Kingston Peak Formation, Death Valley, California. *Geology*, **27**, 339–342.

Rainbird, R. H., Hearnan, L. M. & Young, G. 1992. Sampling Laurentia: detrital zircon geochronology offers evidence for an extensive Neoproterozoic river system originating from the Grenville orogen. *Geology*, **20**, 351–354.

Rainbird, R. H., McNicoll, V., Theriault, R., Heaman, L., Abbott, J., Long, D. & Thorkelson, D. 1997. Pan-continental river system draining Grenville Orogen recorded by U–Pb and Sm–Nd geochronology of Neoproterozoic quartzarenites and mudrocks, northwestern Canada. *The Journal of Geology*, **105**, 1–17.

Rämö, O. T., McLemore, V. T., Hamilton, M. A., Kosunen, P. J., Heizler, M. & Haapala, I. 2003. Intermittent 1630–1220 Ma magmatism in central Mazatzal province: new geochronologic piercing points and some tectonic implications. *Geology*, **31**, 335–338.

Reading, H. G. 1980. Characteristics and recognition of strike-slip fault systems. *Sedimentation in Oblique-slip Mobile Zones*, **4**, 7–26.

Reid, A. J. & Hand, M. 2012. Mesoarchean to Mesoproterozoic evolution of the southern Gawler Craton, South Australia. *Episodes – News Magazine of the International Union of Geological Sciences*, **35**, 216.

Renik, B. & Christie-Blick, N. 2013. A new hypothesis for the amount and distribution of dextral displacement aliong the Fish Lake Valley–northern Death Valley–Furnace Creek fault zone, California–Nevada. *Tectonics*, **32**, 123–145.

Roberts, M. T. 1982. Depositional environments and tectonic setting of the Crystal Spring Formation, Death Valley region, California: geology of selected areas in the San Bernardino Mountains, western Mojave Desert, and southern Great Basin, California. *In*: Cooper, J. P., Troxel, B. W. & Wright, L. A. (eds) *Western Mojave Desert and Southern Great Basin, California*. Geological Society of America Cordilleran Section Meeting Guidebook, Field Trip 9, Death Valley Publishing Company, Shoshone, CA, 143–154.

Rogers, G., Hyslop, E., Strachan, R., Paterson, B. & Holdsworth, R. 1998. The structural setting and U–Pb geochronology of Knoydartian pegmatites in W Inverness-shire: evidence for Neoproterozoic tectonothermal events in the Moineof NW Scotland. *Journal of the Geological Society*, **155**, 685–696.

Rooney, A. D., Macdonald, F. A., Strauss, J. V., Dudás, F.Ö., Hallmann, C. & Selby, D. 2014. Re-Os geochronology and coupled Os-Sr isotope constraints on the Sturtian snowball Earth. *Proceedings of the National Academy of Sciences*, **111**, 51–56.

Rooney, A. D., Strauss, J. V., Brandon, A. D. & Macdonald, F. A. 2015. A Cryogenian chronology: Two long-lasting synchronous Neoproterozoic glaciations. *Geology*, G36511-1.

Rybczynski, D. 2009. *Correlation, Paleogeography, and Provenance of the Eastern Uinta Mountain Group, Goslin Mountain Area, Daggett County, Northeastern Utah*. MS thesis, Utah State University.

Sears, J. W. & Price, R. A. 2000. New look at the Siberian connection: no SWEAT. *Geology*, **28**, 423–426.

Sears, J. W., Price, R. A. & Khudoley, A. K. 2004. Linking the Mesoproterozoic Belt – Purcell and Udzha basins across the west Laurentia–Siberia connection. *Precambrian Research*, **129**, 291–308.

Serpa, L. & Pavlis, T. L. 1996. Three-dimensional model of the late Cenozoic history of the Death Valley region, southeastern California. *Tectonics*, **15**, 1113–1128.

Shafer, D. C. 1983. *Petrology and Depositional Environments of the Beck Spring Dolomite, Southern Death Valley Region* MS Thesis, University of California at Davis.

Snow, J. K. & Wernicke, B. P. 2000. Cenozoic tectonism in the central Basin and Range: magnitude, rate, and distribution of upper crustal strain. *American Journal of Science*, **300**, 659–719.

Snow, J. K., Asmerom, Y. & Lux, D. R. 1991. Permian–Triassic plutonism and tectonics, Death Valley region, California and Nevada. *Geology*, **19**, 629–632.

Stewart, J. H. 1970. *Upper Precambrian and Lower Cambrian Strata in the Southern Great Basin, California and Nevada*. US Geological Survey, Reston, VA, Professional Papers.

Stewart, J. H. 1975. Initial deposits in the Cordilleran geosyncline: Evidence of a late Precambrian (<850 m.y.) continental separation. *Geological Society of America Bulletin*, **83**, 1345–1360.

Stewart, J. H., Gehrels, G. E., Barth, A. P., Link, P. K., Christie-Blick, N. & Wrucke, C. T. 2001. Detrital zircon provenance of Mesoproterozoic to Cambrian arenites in the western United States and northwestern Mexico. *Geological Society of America Bulletin*, **113**, 1343–1356.

Strauss, J. V., Rooney, A. D., Macdonald, F. A., Brandon, A. D. & Knoll, A. H. 2014. 740 Ma vase-shaped microfossils from Yukon, Canada: implications for Neoproterozoic chronology and biostratigraphy. *Geology*, **42**, 659–662.

Strickland, B. A., Wooden, J. L., Mattinson, C. G., Ushikubo, T., Miller, D. M. & Valley, J. W. 2013. Proterozoic evolution of the Mojave crustal province as preserved in the Ivanpah Mountains, southeastern California. *Precambrian Research*, **224**, 222–241.

Summa, C. L. 1993. *Sedimentologic, stratigraphic, and tectonic controls of a mixed carbonate-siliciclastic succession; Neoproterozoic Johnnie Formation, Southeast California*, PhD thesis, Massachusetts Institute of Technology.

Thorkelson, D. J. 2000. Geology and mineral occurrences of the Slats Creek, Fairchild Lake and 'Dolores Creek' areas, Wernecke Mountains (106D/16, 106C/13, 106C/14), Yukon Territory. *Exploration and Geological Services Division, Yukon, Indian and Northern Affairs Canada. Bulletin*, **10**, 73.

Timmons, J. M., Karlstrom, K. E., Dehler, C. M., Geissman, J. W. & Heizler, M. T. 2001. Proterozoic multistage (ca. 1.1 and 0.8 Ga) extension recorded in the Grand Canyon Supergroup and establishment of northwest-and north-trending tectonic grains in the southwestern United States. *Geological Society of America Bulletin*, **113**, 163–181.

Tucker, M. E. 1982. Precambrian dolomite – petrographic and isotopic evidence that they differ from Phanerozoic dolomites. *Geology*, **10**, 7–12.

Tucker, M. E. 1983. Diagenesis, geochemistry, and origin of a Precambrian dolomite – the Beck Spring Dolomite of eastern California. *Journal of Sedimentary Petrology*, **53**, 1097–1119.

Turner, N., Black, L. & Kamperman, M. 1998. Dating of Neoproterozoic and Cambrian orogenies in Tasmania. *Australian Journal of Earth Sciences*, **45**, 789–806.

Van Breemen, O., Pidgeon, R. & Johnson, M. 1974. Precambrian and Palaeozoic pegmatites in the Moines of northern Scotland. *Journal of the Geological Society*, **130**, 493–504.

Vidal, G. & Ford, T. D. 1985. Microbiotas from the late Proterozoic Chuar Group (northern Arizona) and Uinta Mountain Group (Utah) and their chronostratigraphic implications. *Precambrian Research*, **28**, 349–389.

Walker, J. D., Klepacki, D. W. & Burchfiel, B. 1986. Late Precambrian tectonism in the Kingston Range, southern California. *Geology*, **14**, 15–18.

Wang, X.-L., Zhou, J.-C., et al. 2007. Detrital zircon geochronology of Precambrian basement sequences in the Jiangnan orogen: dating the assembly of the Yangtze and Cathaysia Blocks. *Precambrian Research*, **159**, 117–131.

Wasserburg, G. J., Wetherill, G. W. & Wright, L. A. 1959. Ages in the Precambrian terrane of Death Valley, California. *Journal of Geology*, **67**, 702–708.

Wernicke, B. P., Axen, G. J. & Snow, J. K. 1988. Basin and range extensional tectonics at the latitude of Las Vegas, Nevada. *Geological Society of America Bulletin*, **100**, 1738–1757.

Wooden, J. L., Barth, A. P. & Mueller, P. A. 2013. Crustal growth and tectonic evolution of the Mojave crustal province: insights from hafnium isotope systematics in zircons. *Lithosphere*, **5**, 17–28.

Wright, L. A. 1954. *Geology of the Alexander Hills area, Inyo and San Bernardino Counties*. California Division of Mines and Geology, California, Map Sheet 17.

Wright, L. A. 1976. Late Cenozoic fault patterns and stress fields in the Great Basin and westward displacement of the Sierra Nevada block. *Geology*, **4**, 489–494.

Wright, L. A., Troxel, B. W., Williams, E. G., Roberts, M. T. & Diehl, P. E. 1976. Precambrian sedimentary environments of the Death Valley region, eastern California. *In*: Troxel, B. W. & Wright, L. A. (eds.) *Geologic Features, Death Valley*. California Division of Mines and Geology, Sacramento, CA, 7–15.

Wright, L. A., Thompson, R. A., et al. 1991. Cenozoic magmatic and tectonic evolution of the east-central Death Valley region, California. *In*: Walawender, M. J. & Hanan, B. B. (eds) *Geological Excursions in Southern California and Mexico, Field Trip Guidebook*. Geological Society of America, Boulder, CO, 93–127.

Wright, L. A., Troxel, B. W. & Prave, A. R. 1992. Field traverse of Proterozoic rock units, Alexander Hills and southern Nopah Range, Death Valley region, CA. *In*: *Geological Society of America Penrose Conference: Late Precambrian Plate Tectonics and the Dawn of the Phanerozoic*. Geological Society of America, Boulder, CO, 1–11.

Yonkee, W., Dehler, C., et al. 2014. Tectono-stratigraphic framework of Neoproterozoic to Cambrian strata, west-central US: protracted rifting, glaciation, and evolution of the North American Cordilleran margin. *Earth-Science Reviews*, **136**, 59–95.

Zempolich, W. G., Wilkinson, B. H. & Lohmann, K. C. 1988. Diagenesis of late Proterozoic carbonates – the Beck Spring Dolomite of eastern California. *Journal of Sedimentary Petrology*, **58**, 656–672.

Zhao, J.-H., Zhou, M.-F., Yan, D.-P., Zheng, J.-P. & Li, J.-W. 2011. Reappraisal of the ages of Neoproterozoic strata in South China: no connection with the Grenvillian orogeny. *Geology*, **39**, 299–302.

Zhou, M.-F., Yan, D.-P., Kennedy, A. K., Li, Y. & Ding, J. 2002. SHRIMP U–Pb zircon geochronological and geochemical evidence for Neoproterozoic arc-magmatism along the western margin of the Yangtze Block, South China. *Earth and Planetary Science Letters*, **196**, 51–67.